Nano Research

ISSN 1998-0124 CN 11-5974/O4
https://doi.org/10.1007/s12274-023-6169-x

Review Article

Carbon-based functional materials for atmospheric water utilization

Wenya He, Tengyu Lin, Huhu Cheng (✉), and Liangti Qu (✉)

Laboratory of Flexible Electronics Technology, Key Laboratory of Organic Optoelectronics & Molecular Engineering, Ministry of Education, Department of Chemistry, State Key Laboratory of Tribology in Advanced Equipment (SKLT), Tsinghua University, Beijing 100084, China

Received: 4 August 2023 / **Revised:** 5 September 2023 / **Accepted:** 6 September 2023

ABSTRACT

Atmospheric water, as one of the most abundant natural resources on Earth, has attracted huge research interest in the field of water harvesting and energy harvesting and conversion owing its environmental friendliness and easy access. The developments of new materials have seen advanced technologies that can extract water and energy out of this long-neglected resource, suggesting a promising and sustainable approach to address the water and energy crises over the world. Carbon-based functional materials have been considered to be indispensable materials for atmospheric water utilization due to their large surface area, excellent adsorption performance, and higher surface activity. In this review, first, we analyze the interaction between carbon-based functional materials and atmospheric water molecular. Then, technologies developed in recent years for atmospheric water utilization based on carbon-based functional materials are reviewed, mainly focusing on atmospheric water harvesting, moisture-enabled electricity generation, and moisture-responsive actuation. Finally, the remaining challenges and some tentative suggestions possibly guiding developments are proposed, which may pave a way for a bright future of carbon-based functional material in the utilization of atmospheric water.

KEYWORDS

carbon-based functional material, atmospheric water, atmospheric water harvesting, moisture-enabled power generator, moisture actuators

1 Introduction

Since the demand for water and energy has increased as a result of population increase, industrialization, urbanization, environmental degradation, and climate change, seeking easily accessible water and sustainable clean energy for human survival has become one of the important issues concerned by the whole society [1–5]. Atmospheric water is omnipresent in the air regardless of geographical or hydrologic circumstances, and plays an important part in the global hydrologic cycle since it contains enormous volumes of water and energy [6, 7]. Therefore, exploring advanced technologies that can collect water and energy from this long-neglected resource suggests a potential and sustainable strategy to address the water and energy crisis.

With the developments of functional materials, advanced technologies of extracting water and energy out of atmospheric water based on interaction between functional materials and atmospheric water molecular have materialized in recent years, suggesting a promising approach to address the water and energy crises. These technologies include atmospheric water harvesting which refers to the direct generation of water from moisture, and energy harvesting by moisture-enabled electricity generators and actuators which transfer chemical energy from moisture diffusion into electrical or mechanical energy via the interaction between moisture and a variety of materials [8–10]. For water harvesting, functional materials can capture the water molecular from ubiquitous moisture via absorption or adsorption, which refers to the attachment of water molecules to materials through physical or chemical processes (Figs. 1(a) and 1(b)) and releasing water during desorption stage. Energy harvesting based on interaction between functional materials with water molecular in atmospheric moisture mainly involved in process of water adsorption and solvation effect induced ions dissociation and diffusion (Fig. 1(c)). By artificially constructing asymmetrical material components or device structures, a concentration gradient of dissociated charge carriers can form across the material, leading to an induced potential between two electrodes [11–14]. Besides, the interaction between atmospheric water and functional materials will induce material deformation (Fig. 1(d)), usually swelling during water adsorption and shrinking during dehydration, achieving energy harvesting and conversion [15, 16]. In these processes, the properties of functional materials should be considered and meet the following requirements: affinity to moisture, which affects the adsorption capacity of material; rich in polar oxygen-containing functional groups, which enables the material to capture water molecules from air through hydron bonding and provides the dissociated ions during hydration; specific surface area, which determines the number of adsorption sites available on sorbents; pore features including pore size, distribution, and connectivity, which affects the kinetics of adsorption/desorption, speed of mass exchange, and the adsorption capacity; and thermal/electrical conductivity, which facilitates heat exchange, charge transfer, and the adsorption/desorption of water molecular.

Address correspondence to Huhu Cheng, huhucheng@tsinghua.edu.cn; Liangti Qu, lqu@mail.tsinghua.edu.cn

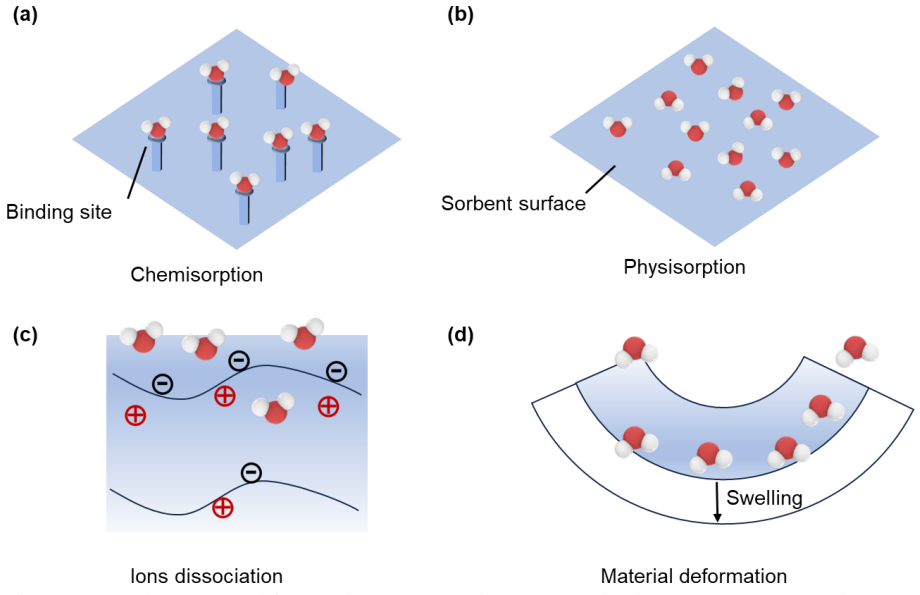

Figure 1 The interaction between atmosphere water and functional materials. (a) Chemisorption. (b) Physisorption. (c) Water adsorption induced ions dissociation and diffusion. (d) Water adsorption induced functional material deformation.

Based on the abundant nanoscale morphologies, high surface area, good electrical conductivity, easily regulation chemistry characters, diverse macroscopic assemblies, and fast adsorption and desorption kinetics, carbon-based functional materials (e.g., active carbon, carbon nanotube, graphene, and their derivatives) have been considered to have key factors mentioned above and demonstrate promising capacity for atmosphere water utilization [17–21]. In this review, first, we set forth th basic mechanism of interaction between carbon-based functional materials and atmosphere water molecular. Then, technologies developed in recent years to water and energy harvesting from moisture based on carbon-based functional materials are reviewed, mainly focusing on atmospheric water harvesting, moisture-enabled electricity generation, and moisture-responsive actuation. Finally, the remaining challenges and some tentative suggestions possibly guide developments of carbon-based functional materials for atmosphere water utilization, assisting in addressing the water and energy crises in future.

2 The interaction of carbon-based functional materials with atmospheric water

Carbon, an abundant element in the universe and on Earth, widely exists in different allotropes for natural and artificial materials [22]. The discovery of fullerene in 1985 has opened a new branch of carbon chemistry, covering various types of carbon nanostructures such as carbon nanotube (CNT), graphene, graphdiyne, and their derivatives [23–30]. Because of excellent chemical stability, good electrical conductivity, large specific surface area, unique porosity, and multifarious structure, carbon-based functional materials have attracted extensive research interest in adsorption [31–33], electrochemistry [34–36], catalyst [37–40], pollutant removal [41–44], biosensing [45], storage and conversion [46–52], and electronic device [53–54].

For atmospheric water utilization, large specific surface area of carbon-based materials provides huge contact space with water molecules firstly. Second, easily-regulated groups including oxygen-containing functional groups or functional nanomaterials benefit water adsorption process greatly, as well as the enormous capillary force formed by the nanoscale confined space. Third, diverse macroscopic assemblies (e.g., foam, film, and fiber) bring a variety of and unusual microstructures for improving inner charge transfer and improve the corresponding kinetics of water adsorption/desorption process. The primary adsorption active sites for water molecules on carbon-based functional materials are assumed to be oxygen-containing functional groups, which determine how water adsorption begins [55–58]. The concentration and type of oxygen-containing functional group as well as their location and distribution on the surface of carbon-based functional material significantly influence the water adsorption behaviors [59–61]. Besides, the adsorbed water molecules can act as nucleation sites for further adsorption of water via hydrogen bonds, which eventually induces hydration layers and water clusters on the surfaces or pores of carbon-based functional material. So, the water adsorption on carbon-based functional material is also affected by surface structure and pore structure such as pore size distribution and the pore connectivity [62–66]. These benefits have encouraged the utilization of carbon-based functional materials for atmospheric water harvesting, moisture-enabled electricity generation, and moisture-responsive actuation.

3 Carbon-based functional materials for atmospheric water harvester

Atmospheric water harvesting (AWH) technology, as one of the decentralized strategies for freshwater generation, has the potential to provide flexible, distributed, community-managed, off-grid access to safe, and potable water, particularly in areas where water scarcity is geographically or economically presented [67–70]. There are different ways for AWH such as fog collection by using large nets to capture water droplets suspended in air, cooling air below its dew point to collect water, and sorbent-assisted harvesting by chemical or physical processes adsorption process. Sorbent-assisted AWH demonstrates superiority in terms of applicability to a wide variety of climates and geographies, water production, and energy efficiency, which includes following processes: moisture capture, water releasing, and collecting. These processes can be regulated by optimizing the physical or chemical interactions between water and sorbent materials. In this section, we mainly introduce the application of carbon-based functional materials in AWH technology and ways to improve the kinetics of water adsorption/desorption for highly efficient water harvesting in order to clarify the relationship between material structure and performance of atmospheric water harvester.

The extremely easy functionalization of carbon-based

functional materials makes them useful for improving the performance of AWH through the introduction of oxygen-containing functional groups. Graphene oxide (GO) possesses rich oxygen-containing functional groups like carboxyl (–COOH), and hydroxyl (–OH) confers important role for the AWH based on the interaction between surface functional group and water molecule [71–73]. As shown in Fig. 1(b), due to the larger proportion of hydrophilic functional groups, membrane-like GO prepared by vacuum filtration exhibits high water adsorption capacity, which is at least two times higher than that of a conventional desiccant material such as silica gel across the tested range of relative pressure [71].

Oxygen-containing functional groups, which determine how water adsorption begins, can profoundly change the adsorption behaviors of carbon-based materials. Thus, the water adsorption properties can be further regulated by the modification of other carbon-based functional materials with different kinds of functional group. Huang and co-workers adopted a low temperature oxygen plasma technology to introduce oxygen-containing functional groups on surface of activated carbon fibers (ACFs), which increases carbon atoms with unpaired electrons as active sites to improve moisture adsorption, lighting on the potential application in harvesting water from air at low relative humidity [74]. Kim and workers also demonstrated that oxygen functional groups on activated carbon (AC) surface play a critical role for moisture adsorption [75]. The surface functionalities, in particular –COOH and sulfonic acid (–S=O) functional groups on carbon surface, may govern the adsorption of moisture at low relative humidity (RH); while the other types of oxygen functional groups, such as –OH, may contribute to the adsorption of moisture at medium or high RHs. Therefore, optimizing the functional groups on surface of carbon-based functional materials would be an effective strategy to improve the performance of water adsorption for productive water harvesting.

In addition, based on high specific evaporation surface area, excellent photothermal property, and thermal conductivity, carbon-based functional materials have been demonstrated to incorporate with hygroscopic materials including polymer hydrogels [76], hygroscopic salts [77–80], and MOFs [81, 82] as composite moisture-harvesting materials to further improve moisture adsorption capacity and promote the desorption process driven by natural sunlight or low-grade waste heat for efficient atmospheric water harvester. For example, Wang and coworkers developed a polyacrylamide (PAM)-CNT-$CaCl_2$ hybrid composite (Fig. 2(a)) with outstanding water adsorption capability as an effective photothermal water sorbent for AWH [76]. CNT is used as the photothermal component due to its chemical stability, superior light absorbance and outstanding light-to-heat conversion efficiency as demonstrated in Refs. [83, 84]. With RH increasing from 10% to 80%, the water uptake of PAM-CNT-$CaCl_2$ samples increases from 5% to 173% (Fig. 2(b)). At an outdoor experiment, the device quickly delivered ~ 20 g of fresh water within just 2.5 h under natural sunlight, demonstrating its promising for practical application. Wang and co-workers [79] introduced an atmospheric water generator using GO-based aerogel with a high-concentration liquid sorbent ($CaCl_2$ 50 wt.% solution) system that enables efficient and effective desorption out of the sorbent through interfacial heating during day time (Figs. 2(c) and 2(d)). As a result, fresh water (2.89 $kg{\cdot}m^{-2}{\cdot}day^{-1}$) can be produced at about 70% RH, with only solar energy input and energy efficiency of desorption as high as 66.9%. Recently, Hu and coworkers [81] prepared CNTs decorated hollow MIL-101(Cr) (HMC) particles for solar-driven atmospheric water harvesting with nice water adsorption capacity and fast kinetics (Fig. 2(e)). The composites achieved a maximum water uptake of 1.074 $g{\cdot}g^{-1}$ at 90% RH and the water adsorption capacity at low humidity (40% RH) is 113% higher than that of pure MIL-101 (Fig. 2(f)). These progresses prove that synergistic functions of carbon-based functional material with other hygroscopic materials significantly promote the performance of AWH.

Rational structure optimization of carbon-based composites can further improve the adsorption/desorption kinetics of water molecules, so as to achieve more efficient AWH device. Yao and co-workers demonstrated a highly efficient clean water production system based on a rationally designed sodium polyacrylate (PAAS)/graphene framework (PGF) [85]. As shown in Fig. 3(a), PAAS is well dispersed in a GO dispersion and through a freeze-drying process as well as reduction under the vapor of $N_2H_4{\cdot}H_2O$ to obtain PGF with homogeneous microporous structure with a pore size ranging from 30 to 50 μm and porosity of up to 99%. The microporous structure of PGF provides effective transport channels and an enlarged contact area for moisture, and oxygen functional groups of PAAS can spontaneously capture water molecules through hydrogen bonding. As a result, the water sorption capacity of PGF is 5.20 $g{\cdot}g^{-1}$ at RH of 100% and 0.14 $g{\cdot}g^{-1}$ at a low RH of 15%, which is outstanding compared with all the previous work. And the PGF-based AWH device presents the potential for practical application of water harvest of over 25 $L{\cdot}kg^{-1}$ of PGF daily (Figs. 3(b)–3(d)), enough to meet several people's drinking water demand, demonstrating a new way for clean water production from naturally variable atmospheric environments. Xu and co-workers [86] reported a nanocomposite sorbent with vertically aligned structure by confining lithium chloride (LiCl) in a reduced graphene oxide (rGO) and sodium alginate (SA) matrix (LiCl@rGO-SA) (Fig. 3(e)). The sorbent shows high water uptake, as high as thrice its weight. Moreover, LiCl@rGO-SA exhibits fast sorption–desorption kinetics enabled by the vertically aligned and hierarchical pores of the rGO-SA matrix as moisture transfer channels (Fig. 3(f)). To demonstrate its practical application, a scalable solar-driven rapid-cycling continuous atmospheric water harvester with synergetic heat and mass transfer enhancement was developed, realizing eight continuous water capture-collection cycles per day and ultrahigh water productivity up to 2120 $mL_{water}{\cdot}kg_{sorbent}^{-1}{\cdot}day^{-1}$ from dry air without any other energy consumption. Very recently, lithium chloride-incorporated holey graphene aerogel fiber (LiCl@HGAFs) with highly efficient moisture capture is reported by Hou and co-workers [80]. Holey graphene aerogel fiber was prepared via wet spinning, HI reduction, and supercritical drying. LiCl was introduced by simple impregnation. The holey graphene aerogel porous matrix provides not only sufficient binding sites and surface area for water uptake but also abundant water transport pathways through the etched nanopores. As a result, LiCl@HGAFs realized the water sorption capacity over 4.15 $g{\cdot}g^{-1}$ and multiple pathways to perform sorption/desorption processes.

As mentioned above, thanks to the adjustable structures and excellent properties of carbon-based functional materials, many great processes have been made in the field of AWH technology. The researchers optimized properties of the carbon-based functional materials absorbent through surface modification, structure design, and materials compositing, which improved the water molecule capture ability of material and accelerated kinetics of adsorption/desorption in AWH technology. These strategies significantly enhance the performance of AWH device, which makes it more accessible for efficient water production.

4 Carbon-based functional materials for moisture-enabled electricity generator

Moisture-enabled power generator (MEG), which harvests energy from atmospheric water in humidity air to provide economical and sustainable electricity, has advanced quickly and is gaining

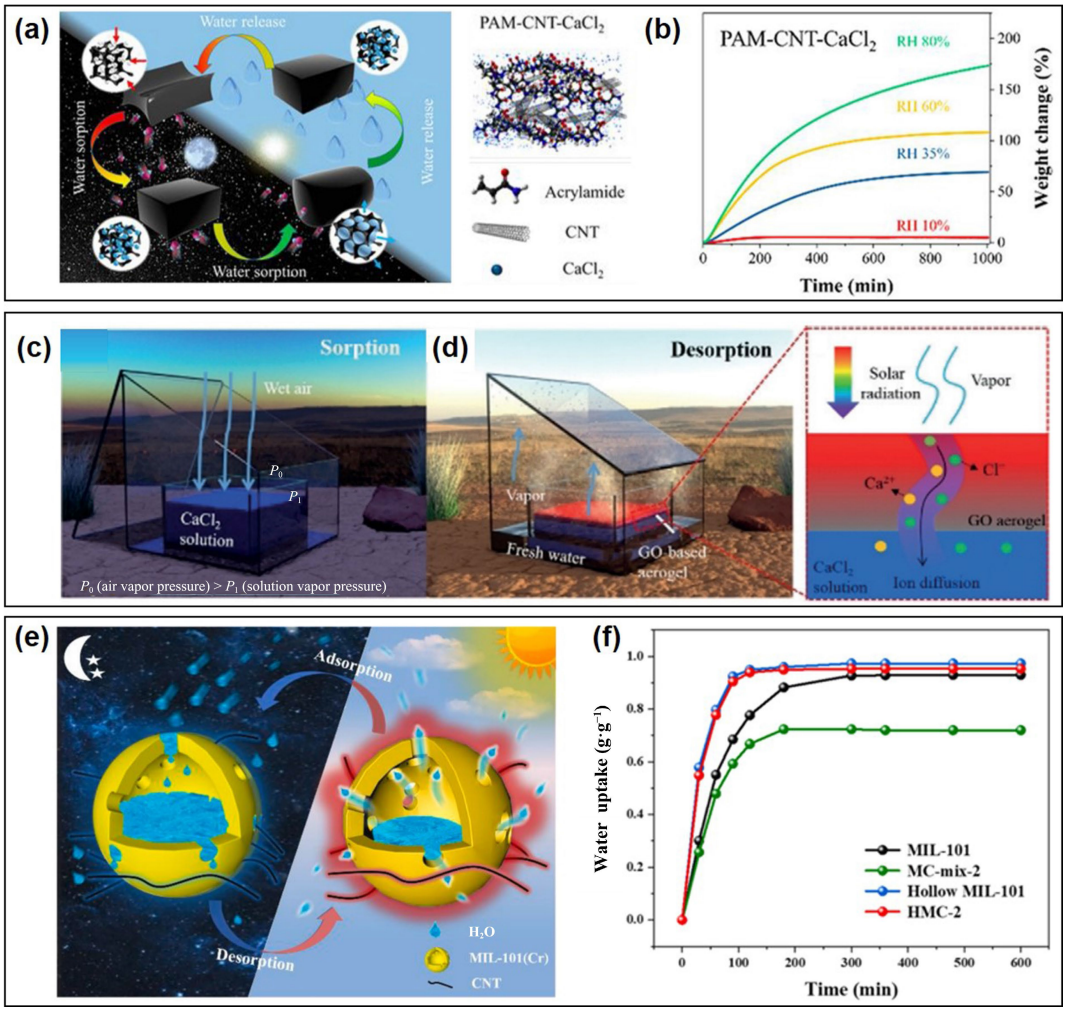

Figure 2 (a) Conceptual design of the hybrid hydrogel (PAM-CNT-$CaCl_2$). (b) Moisture sorption curves of PAM-CNT-$CaCl_2$ at different relative humidity. Reproduced with permission from Ref. [76], © American Chemical Society 2018. (c) Moisture sorption on GO-based aerogels with $CaCl_2$ at nighttime. (d) Water desorption during the daytime under sunlight and the structures of the GO-based aerogel as a salt-resistant absorber during solar water desorption. Reproduced with permission from Ref. [79], © WILEY-VCH Verlag GmbH & Co. KGaA, Weinheim 2019. (e) Illustrating the water harvesting from air process for HMC composites. (f) Time dependent water uptake of different composites at 25 °C and 80% RH. Reproduced with permission from Ref. [81], © Elsevier B.V. 2021.

popularity due to their wide range of possible applications [87–92]. In MEG, gaseous water molecules in moist air are captured by the functional groups of hygroscopic films such as –OH, –COOH, and $–SO_3H$, and converted into liquid water to release chemical energy, which subsequently leads to the dissociation and migration of mobile ions, giving rise to electric voltage and current. Thus, by combining moisture, electrodes, and specially formulated hygroscopic films, electricity may be extracted straight from the atmosphere in this way. Since the proposed GO-based MEG devices in 2015 [93], this technology has been rapidly developed, and a series of functional materials have been developed. Carbon-based functional materials and their derivatives are of significant interest for the construction of MEG devices for the production of electricity through water adsorption and proton diffusion because of their readily controlled functional groups that are abundant in hydrophilic oxygen-containing functional groups. Moreover, macroscopic assemblies of carbon-based functional materials including quantum dot (zero-dimensional (0D)), fiber or nano ribbon (one-dimensional (1D)), film (two-dimensional (2D)), and foam (three-dimensional (3D)) provide favorable advantages for high-performance and diversified MEG systems.

The intrinsic small size, high specific surface area, and abundant edge sites of carbon-based quantum dot provide an avenue to good adsorption of moisture and transportation of hydrated ions during MEG process, thus offering exciting opportunities to achieve output performance of power generation. For example, a high-performance moisture triggered nanogenerator is fabricated by Huang and co-workers using graphene quantum dots (GQDs) as the active material [94]. GQDs with oxygen-containing functional groups were prepared by oxidation of natural graphitic powder (Fig. 4(a)) and the GQDs-based MEG was pre-treated with an electrochemical polarization to establish an oxygen-containing functional groups gradient for electricity generation. Easy moisture absorption could be realized at the edges and defects of GQDs and diffusion through the functional layer along thickness direction, mainly owing to their tiny sizes and large specific surface area (Fig. 4(b)). As a result, the device can deliver a high voltage up to 0.27 V under 70% relative humidity variation (Fig. 4(c)). Li and coworkers [95] reported a flexible MEG device by directly printing carbon dots (CDs) on paper and a simple method for self-establishing an ionic gradient on both sides of the device by creating an asymmetric structure (one side of the device is encapsulated) (Fig. 4(d)), which avoids the need for pre-processing the materials in order to create asymmetric functional groups. Due to the difference in the concentration of the released protons on the two sides, the carboxyl groups on CDs on the open side of the device ionize more protons than those near the closed side, potentially causing a decrease across the device (Fig. 4(e)). The device can produce a sustainable voltage of 40 mV for over

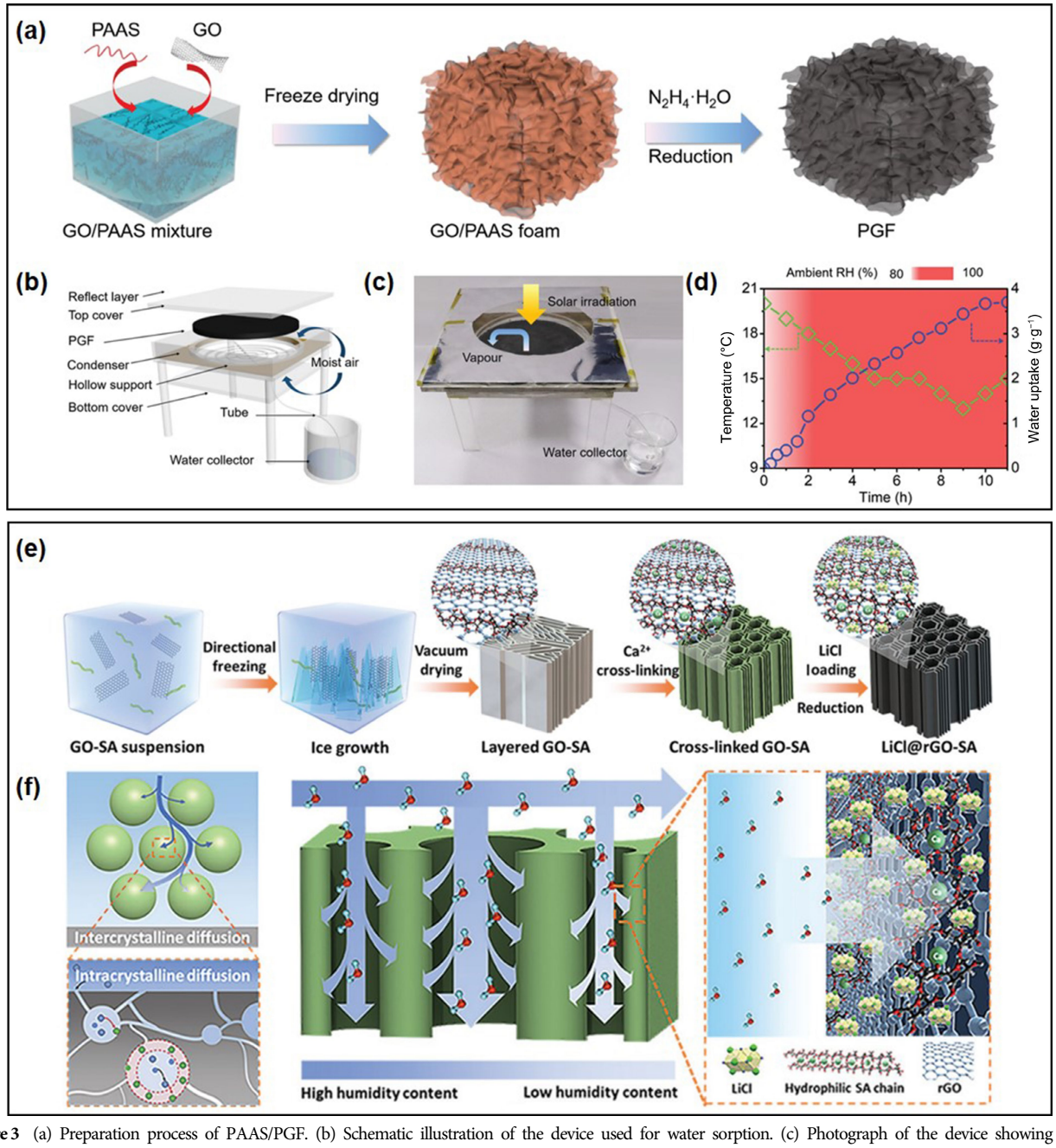

Figure 3 (a) Preparation process of PAAS/PGF. (b) Schematic illustration of the device used for water sorption. (c) Photograph of the device showing water collection. (d) Real-time changes in temperature, humidity, and water uptake in outdoor water sorption experiments. Reproduced with permission from Ref. [85], © WILEY-VCH Verlag GmbH & Co. KGaA, Weinheim 2019. (e) A schematic of the synthesis route for vertically aligned nanocomposite sorbents (LiCl@rGO-SA). (f) Schematic of moisture transport pathways from ambient air to the vertically aligned nanocomposite sorbent. Reproduced with permission from Ref. [86], © The Royal Society of Chemistry 2021.

100 min at a fixed humidity value. In addition, the device responds to direct touching of a finger or human exhalation, thus indicating its great potential for applications in electronic skins and humidity sensors.

Fiber-shaped MEG devices that can be directly woven into textile fabrics for wearable electronics have attracted great attention [96–100]. GO nanosheets with plenty of oxygen-related groups that can be assembled into the fibers through the highly oriented arrangement of GO sheets were used for constructing fiber-shaped MEG device. Liang and coworkers [96] reported a high-performance graphene fiber power generator (GF-Pg) based on GO fiber (Fig. 5(a)). GF-Pg was fabricated by well-controlled region-selective laser irradiation along the GO fiber to form the reduced GO (RGO) electrodes (Fig. 5(b)). The GF-Pg has highly oriented GO sheets assembled within the fiber, which provide favorable channels for efficient ion transport and thus harvests energy from the moisture (Fig. 5(c)). A single fiber generator unit with a length of less than 1 mm and a diameter of 80 μm can generate a voltage of 0.35 V in response to the humidity variation, which could be enhanced to 1.3 V by simply increasing the number of device units. As a result, this moisture-enabled self-powered fiber could be integrated into flexible textiles to realize an information storage/expression, demonstrating the promising applications in wearable electronics. Subsequently, Shao and co-workers [98] also developed a coaxial fiber-shaped MEG based on core silver wire as one electrode, covered with a power generation shell of GO layer and then twined with another silver wire as the counter electrode (Figs. 5(d) and 5(e)). The unique coaxial architecture enables the moisture to diffuse directionally across GO layer, thus leading to the directional movement of ionized H^+ (Fig. 5(f)). Consequently, the as-prepared fiber-shaped MEG device produces a power density of 0.21 μW·cm^{-1} under moisture

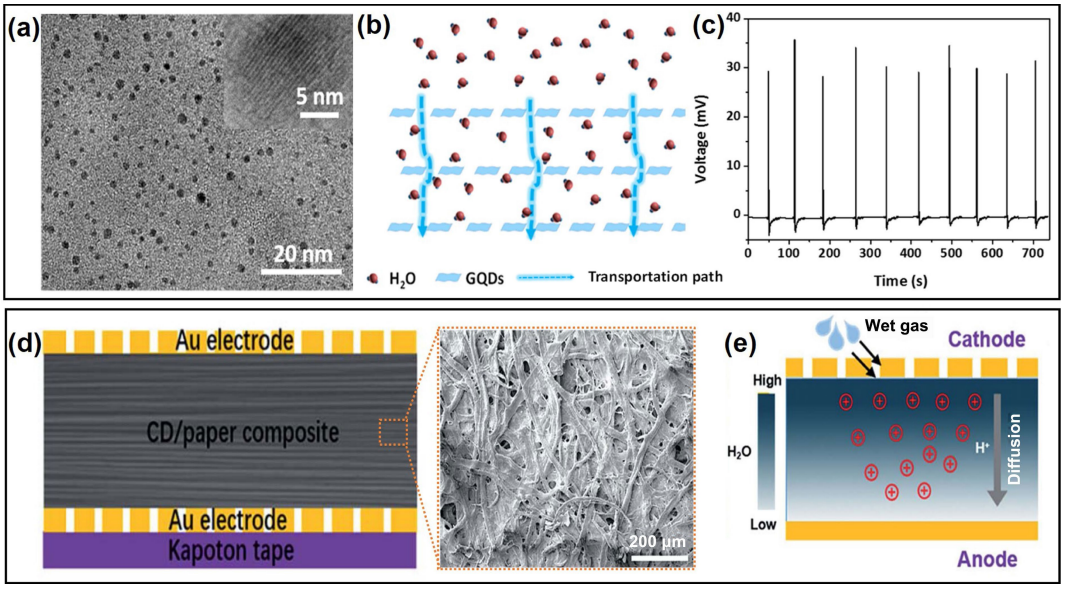

Figure 4 Carbon-based quantum dots materials for MEG. (a) Transmission electron microscopy (TEM) image of GQDs. The inset is the corresponding high-resolution TEM image. (b) Schemes of moisture transportation behavior on GQDs film. (c) Voltage output cycles of a typical gradient GQDs based MEG. Reproduced with permission from Ref. [94], © American Chemical Society 2017. (d) Cross-sectional diagram of CDs/paper-based MEG device and scanning electron microscopy (SEM) image of CDs/paper. (e) Schematic diagram of electricity-generating process of CDs/paper-based MEG device. Reproduced with permission from Ref. [95], © The Royal Society of Chemistry 2018.

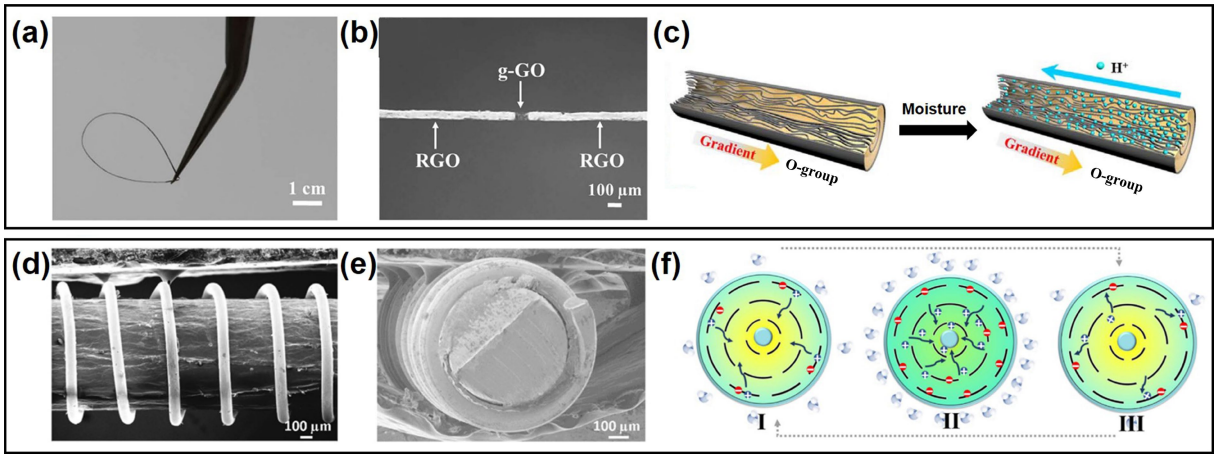

Figure 5 Carbon-based fiber materials for MEG. (a) Photograph and (b) optical microscope image of the GF-Pg. (c) The hydrogen ions were ionized under moisture, and the hydrogen ions diffused from the oxidized end to the reduced end. Reproduced with permission from Ref. [96], © Elsevier Ltd. 2017. (d) Top-view SEM image of the coaxial fiber-shaped MEG. (e) Cross-section SEM image of the coaxial fiber-shaped MEG. (f) Schematic illustration of the power generation mechanism of the coaxial fiber-shaped MEG. Reproduced with permission from Ref. [98], © Elsevier Ltd. 2018.

stimulation. Moreover, the extraordinary shaping ability of the device gives it more morphological possibilities of various shapes, indicating the potential applications for wearable and self-powered electronics.

Carbon-based film materials were widely used in configuration of MEG device, which can be fabricated with significantly increased active materials loading and enlarged electrode size for improving the performance and achieving large-scale production [101–114]. For example, Liu et al. [102] reported a porous carbon film (PCF) MEG with a higher content of oxygen-containing groups on one half and reduced content on the other half by plasma treatment (Figs. 6(a)–6(c)). It is demonstrated that vapor adsorption in the PCF with dissimilar amounts of proton-donating groups on the two sides can directly create significant electrical potential, as a result, this PCF based-MEG exhibits an output voltage of 68 mV, stimulated by 95% RH. Cheng and co-workers [103] demonstrated a flexible in-plane moisture-electric converter (IPMEC) by using a large-scale GO film as active part and *in-situ* laser reduced GO as electrodes, rendering it highly flexibility, and greatly promoting the touchless interface formation between this device and biological moisture sources. The significant role of asymmetric oxygen-containing groups in carbon material is noticeable in MEG devices. It is expected that other functionalized carbon-based functional materials can produced similar results. Lee and co-workers directly fabricated a MEG device by laser-induced graphitization with a gradual defocusing method [105]. As shown in Fig. 6(d), a cellulose substrate was placed on the sample stage of a computer-controlled CO_2 laser engraver with a stage tilted at 56° to fabricate a graphitic carbon film (GCL) with gradient oxygen-to-carbon (O/C) ratio (Fig. 6(e)). The hydrogen-containing groups (carboxyl and hydroxyl groups) in the GCL substrate were hydrolyzed when they were exposed to moisture, and the preexisting O/C gradient caused a density gradient of hydrogen ions to be induced. At a relative humidity of 70%, the resultant outputs of voltage and current were 0.23 V (Fig. 6(f)) and 0.4 A·cm^{-2} (Fig. 6(g)), respectively.

Except above planar structure, Liang et al. [106] demonstrated asymmetric moisturizing induced layer-packed power generation by directly printing the GO onto a moisture insulation substrate

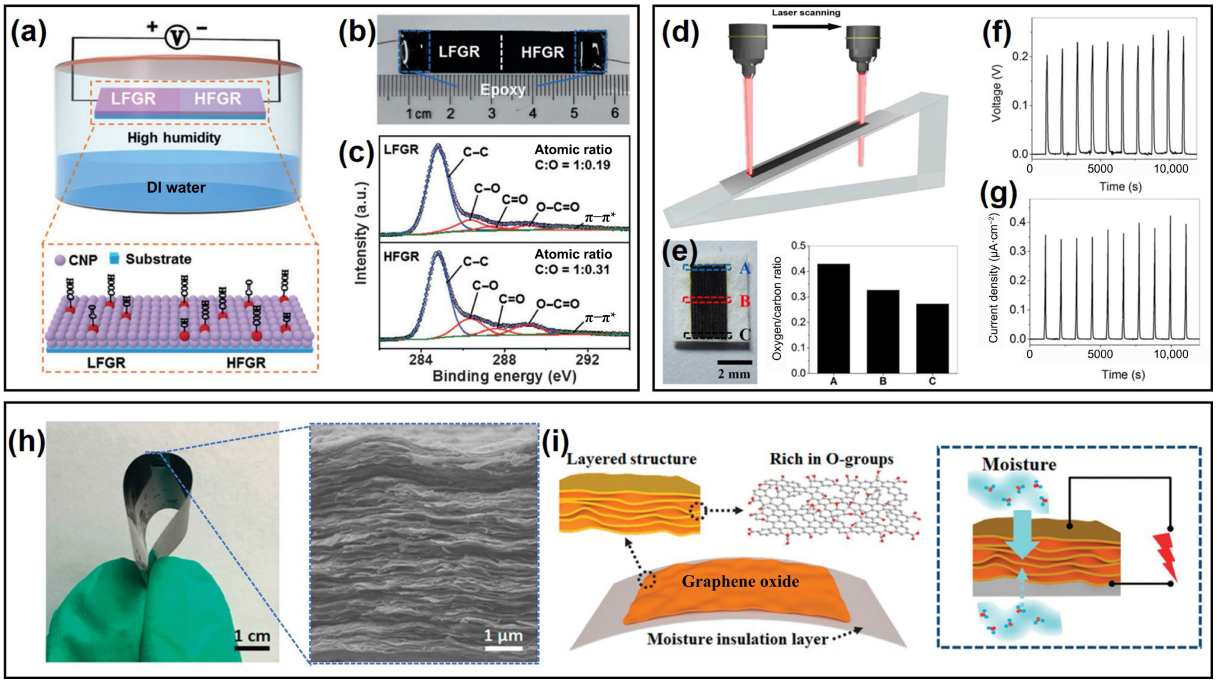

Figure 6 Carbon-based film materials for MEG. (a) A schematic of Experimental setup. (b) Carbon film device. HFGR denotes the region functionalized by plasma treatment, where LFGR denotes the untreated region, and HFGR denotes treated region. (c) X-ray photoelectron spectroscopy (XPS) spectra of the plasma-functionalized (top) and pristine (bottom) region of PCF. Reproduced with permission from Ref. [102], © WILEY-VCH Verlag GmbH & Co. KGaA, Weinheim 2016. (d) Schematic diagram of fabricating a GCL film. (e) Optical image of GCL film and corresponding O/C ration at each section. (f) Voltage and (g) current density output of GCL film at 70% RH. Reproduced with permission from Ref. [105], © American Chemical Society 2019. (h) Bending performance of the GO film and cross-section SEM image of GO showing well-ordered stacking. (i) Schematic diagram of the generator consisting of GO and a moisture insulation layer. Reproduced with permission from Ref. [106], © The Royal Society of Chemistry 2018.

(MIS) (Fig. 6(h)). Due to the presence of the MIS, GO nanosheets at the naked side of a GO/MIS bilayer film may be successfully moistened by moisture exposure, while the moisture from the other side is severely hindered by the MIS, leading to electricity generation (Fig. 6(i)). By customizing the connection between the GO/MIS bilayer films, the self-charging inductive voltage output can be increased to over 2 V, which is sufficient to power commercial electronic devices. This work demonstrates a low-cost, scalable, lightweight, and bendable power generation device, opening up new possibilities for significantly expanding the application areas of carbon material and reducing the cost of portable electronics.

The porous structure of a 3D carbon-based foam can strongly facilitate the diffusion of water molecules and the dissociation of free H^+ ions to produce higher electrical power [115–120]. Zhao et al. investigated the moisture power generation performance of 3D GO assemblies [115]. The GO nanosheets were assembled into 3D porous aerogel foams by freeze-drying, and a functional group gradient structure inside the foam materials (g-3D-GO) was constructed by using electrochemical polarization (Fig. 7(a)). On the basis of the g-3D-GO with gradient oxygen-containing groups and rich pore architecture (Fig. 7(b)), the g-3D-GO-based MEG device produced a high output with a power density of 1 $mW·cm^{-2}$ and an energy-conversion efficiency of 52% under the tidal moisture. Similar configuration is also demonstrated by Cheng and co-workers [116], where an asymmetric porous 3D GO material (a-GOM) was prepared by a directionally-induced thermal reduction strategy (Fig. 7(c)). Importantly, benefiting from the functional groups-reconfiguration and inner protons asymmetrical distribution similar to cell membranes (Fig. 7(d)), a-GOM can proactively generate a sustained electrical voltage of up to 0.45 V in the air. And a soft power generation package can be constructed by orderly assembly of a-GOM in series with flexible electrodes, which can be conveniently folded to fit in pockets as a portable power source. Besides, based on above excellent characteristic of 3D GO bulk, Huang et al described a novel device consisting of a hygroscopic GO bulk with a heterogeneous structure and well-matched electrodes [117]. As shown in Figs. 7(e) and 7(f), the heterogeneous graphene oxide (h-GO) has an integrated structure with a thick GO layer under the gradient-reduced GO (g-rGO) layer, which is fabricated by directionally controlled laser irradiation. Impressively, because of the effective synergy strategy of heterogeneous reconfiguration of oxygen-containing functional groups on hygroscopic GO and mediation of electrodes/materials interfaces with well-designed Schottky junctions (Fig. 7(g)), the MEG device achieves a high-voltage output approaching 1.5 V. To further improve the 3D GO-based MEG, Huang et al. proposed a hybrid structure consisting of porous GO sheets coupled with an interconnected PAAS network (GO/PAAS) [118]. This hybrid structure contains a higher density of hydrophilic groups resulting in high moisture uptake, enabling ion dissociation at the large number of surface functional groups followed by efficient ion transport. And the GO/PAAS-based device can operate at temperatures between −25 and 70 °C and relative humidities ranging from 5% to 95%, indicating its readily adaptable to a variety of environment conditions.

In summary, based on their excellent properties and easily functionalization as well as variety of assemblies, carbon-based functional materials have been widely used in MEG technology. The devices showed high mechanical flexibility, excellent electricity-generating performance, and remarkable environmental adaptability, demonstrating its promising in practical applications such as the construction of self-powered electronics and the incorporation of MEGs in other next-generation devices.

5 Carbon-based functional materials for moisture-enabled actuator

Actuators as stimuli-sensitive devices that transfer an external stimulus into automatic action have attracted growing

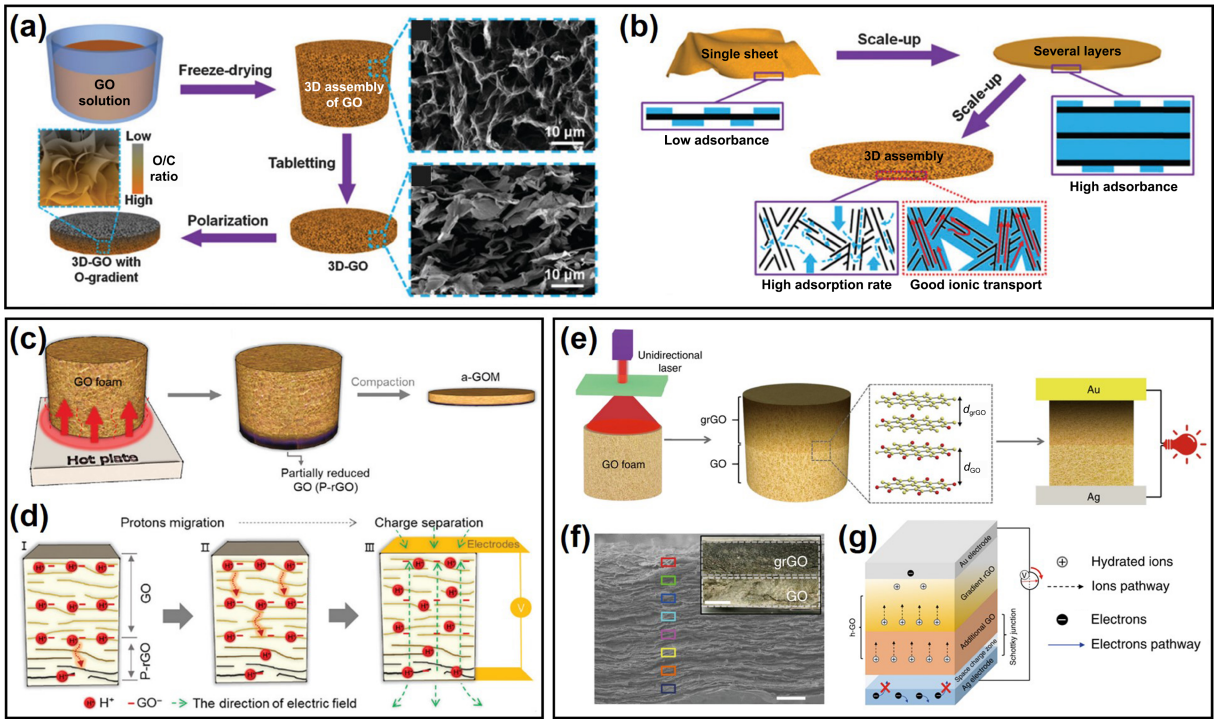

Figure 7 Carbon-based foam materials for MEG. (a) Preparation process of g-3D-GO from GO solution and corresponding SEM images of the porous 3D assembly of GO and the close-grained 3D-GO. (b) Schematic diagram of porous structure assisted fast macroscopic water adsorption of a 3D-GO assembly. Reproduced with permission from Ref. [115], © The Royal Society of Chemistry 2016. (c) Schematic illustration of the preparation of a-GOM. (d) Schematic illustration of the possible mechanism towards spontaneous migration of protons and charge separation in a-GOM under the action of the asymmetric structure. Reproduced with permission from Ref. [116], © The Royal Society of Chemistry 2018. (e) Schematic illustration of the preparation process of h-GO based MEG. (f) Cross-sectional SEM image of h-GO. (g) Well-designed MEG developed with h-GO and well-matched electrodes. Reproduced with permission from Ref. [117], © Huang, Y. X. et al. 2018.

multidisciplinary interest from biology, chemistry, materials science, and engineering [121–124]. Moisture-enabled actuator, which can transform chemical energy activated by moisture into other types of energy upon mechanical deformation, has been widely investigated [125-130]. The main principle for designing moisture-enabled actuator is to combine materials characteristics with structural features. One design strategy is utilizing the difference in hydrophilic capacity between materials with a multilayer or Janus structure to realize the energy conversion and deformation. Another strategy is using same material with composite structure and exploits the structural differences of material or asymmetric moisture adsorption to realize a moisture-enabled deformation. Above all, material selection and structural design are pivotal for moisture actuators to realize preferable performance. On account of their unique tunable microstructures, excellent mechanical performances, and prominent chemical properties, as well as rich oxygen-containing functional groups, carbon-based functional materials such as graphene, GO, functionalized-CNT, or other hybrids have been proven to be a popular choice for moisture-enabled actuators. The assembles includes fiber based actuator, film based actuator, and 3D network based actuator.

Owing to the existence of numerous oxygen functional groups, GO is much more sensitive to moisture. An asymmetric graphene/GO (G/GO) fiber (Fig. 8(a)) was rationally designed by laser-beam irradiation along a pristine GO fiber in 2013 [131]. Remarkably, the G/GO fibers display complex, well-confined, predetermined motion and deformation once exposed to moisture (Fig. 8(b)), demonstrating their application as a single-fiber walking robot. Continuing the effort in developing unconventional applications and exploring the full potential of GO fiber, the intrinsic configuration of graphene within the fiber body was constructed and a new type of moisture-driven rotational motor was achieved by rationally designing the rotary processing of the freshly spun GO fiber hydrogel [132]. Impressively, a twisted GO fiber (TGF) with rearranged graphene sheets within the fibers presents superb performance as a reversible rotary motor, with a rotary speed of up to 5190 rpm and a tensile expansion of 4.7% under humidity alternation.

Importantly, aligned CNT fibers, which have been demonstrated to extend the excellent physical properties of individual CNTs to a macroscopic scale, have been extensively investigated for actuators [133–135]. Thus, Peng and co-workers developed a novel fiber actuators based on aligned CNT fibers with hierarchically helical channels and hydrophilic surfaces (HSFs), which offers a rapid and large contraction and rotation as well as a high reversibility in response to moisture [133]. To prepare HSFs, a pristine aligned CNT fiber was modified with an oxygen plasma treatment and then through a similar twisting process (Fig. 8(c)). In the resulting HSF, a lot of micron-channels formed between the fibers, which makes it accessible in fast response to moisture. By integrating HSFs based actuators, a smart louver was developed, which can response to the change of humidity. As shown in Fig. 8(d), the smart louver was gradually opened with the increasing humidity from 25% to 80% at room, demonstrating its promising for smart device. Kim and coworkers reported a bio-inspired hybrid yarn artificial muscle (HYAM) with a coiled and wrinkled structure by highly twisting a CNT sheet stack that incorporated a hydrophilic poly(diallyldimethylammonium chloride) (PDDA) guest (Fig. 8(e)) [135]. Due to the RH around the HYAM determines the moisture content in the PDDA and the volume of the hybrid yarn, twist or untwist of the yarn within the HYAM occurs as it is exposed to a change in RH (Fig. 8(f)). When the RH was changed from 99% to 10%, the HYAM more quickly fully recovered its initial length by water evaporation in 3 min (Fig. 8(g)). As a result, the water-driven HYAM provides a large tensile stroke (up to 78%), a large gravimetric work capacity (2.17 kJ·kg^{-1}), and high

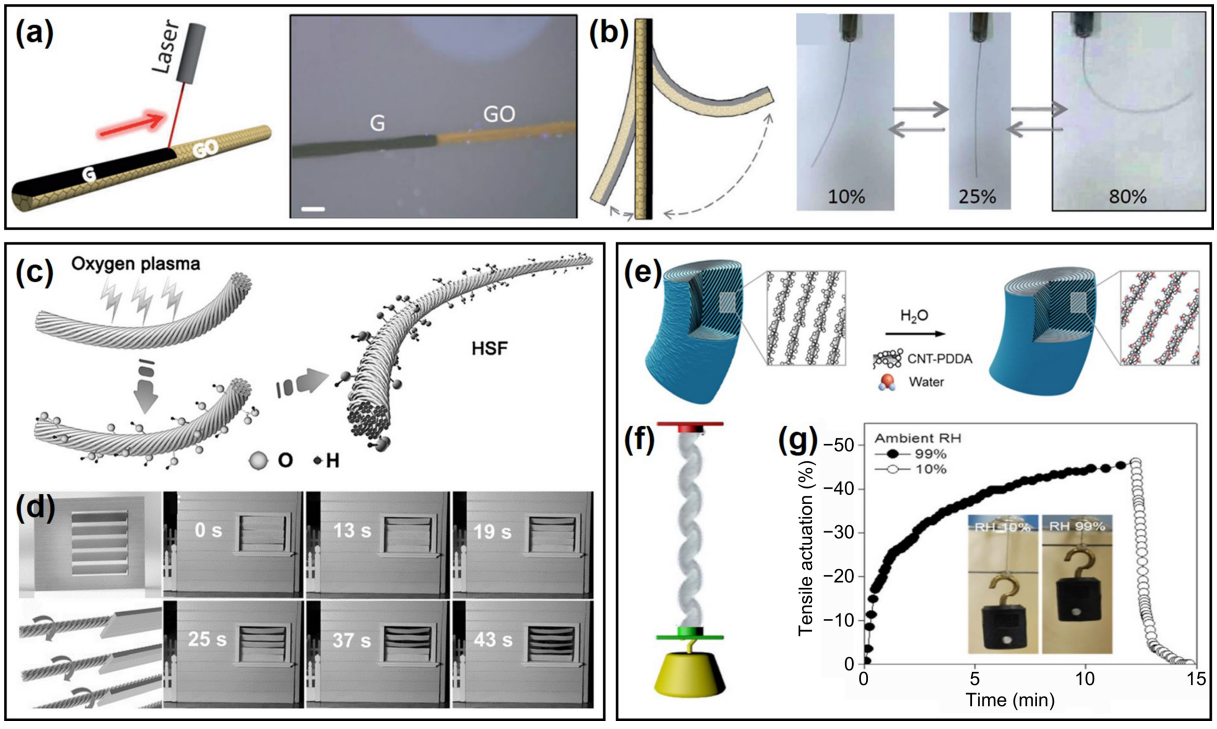

Figure 8 Fiber shaped moisture actuator based on carbon-based functional material. (a) Schematic diagram of fabricating asymmetric G/GO fiber and its photomicrograph. (b) Representation of the possible bending of a G/GO fiber exposed to different relative humidities and corresponding photographs. Reproduced with permission from Ref. [131], © WILEY-VCH Verlag GmbH & Co. KGaA, Weinheim 2013. (c) Fabrication process of HSFs with hierarchically helical channels. (d) Application of HSFs in smart louver in response to moisture. Reproduced with permission from Ref. [133], © WILEY-VCH Verlag GmbH & Co. KGaA, Weinheim 2015. (e) Schematic diagram showing the change in structure of part of the HYAM before and after water absorption. (f) The configuration of a two-end-tethered HYAM. (g) The time dependence of tensile actuation driven by water absorption and desorption. Reproduced with permission from Ref. [135], © Kim, S. H. et al. 2016.

volumetric work capacities (1.8 $MJ \cdot m^{-3}$), which is promising for a moisture driven muscle.

Apart from carbon-based fiber material, 2D carbon assembles were widely investigated for deformable actuators. In 2010, Ruoff and co-workers firstly fabricated a macroscopic actuator based on a GO and COOH-functionalized CNTs (GO/CNT) bilayer film, which exhibits extraordinary actuation in response to changes in humidity [136]. However, during movement, bilayer actuators are vulnerable to weak interlayer adhesion and even layer delamination. To address these problems, the actuators-based homogenous monolayer film or Janus monolayer film has been designed. The sole GO film with an asymmetric surface structure on its two sides has been developed, creating a promising actuation ability triggered by moisture [137]. Ge and co-workers reported a facile strategy for fabricating an actuator driven by moisture gradients based on a homogeneous GO film (Fig. 9(a)) [138]. The homogeneous structure has enabled the actuator to be highly sensitive to the stimuli of humidity gradients (Fig. 9(b)), as well as displaying rapid and continuous motion. Ma and co-workers reported a programmable patterning of RGO/GO Janus paper (Fig. 9(c)) using a threshold-controlled direct laser writing technology [139]. As shown in Fig. 9(d), along the lateral direction after the laser reduction, RGO/GO Janus film presents a significant gradient distribution of oxygen-containing groups. Notably, when combined with a polymer tape, the as-formed tape/RGO/GO structure exhibits reversible moisture-responsive bending deformation, in which the hydrophilic GO layer acts as an active layer for moisture actuation. Due to the photothermal and Joule heating effect of RGO, the device can also be responsive to humidity, light, and electricity (Fig. 9(e)). Moreover, inspired by the natural "quantum-tunneling-fluidics-effect", Zhang and co-workers reported moisture actuation of GO paper with periodic gratings, demonstrating a ultrafast response and large deformation degree [140]. As shown in Fig. 9(f), a unilaterally structured GO film was prepared by soft lithography using poly(dimethylsiloxane) (PDMS) gratings with variable periods as templates folded GO nanosheets that function as quantum-confined superfluidics channels may greatly enhance water adsorption, enabling sensitive and adjustable moisture actuation. To demonstrate its full potential in developing soft robots, the author designed and prepared two kinds of smart GO ribbons with chiral twisting behaviors as legs for assembling a centipede mini-robot (Fig. 9(g)).

Recently, the hybrids consist of carbon-based functional materials and other polymer materials into a 3D network have been proved as a promising way for improving the flexibility of a carbon-based membrane without losing its quick response to moisture, making highly sensitive, flexible, and stable actuators [141–143]. As shown in Fig. 10(a), Xiang and co-workers developed a flexible moisture actuator by evenly dispersing GO sheets into a 3D network combined with polyvinyl alcohol ethylene copolymer nanofibers (PVA-co-PE NFs) and silver nanowires (AgNWs) [141]. The 3D interlaced pore structure of the AgNWs/NFs/GO composite ensured its larger contact area, faster moisture exchange rate, and large bending deformation under moisture stimulation. Additionally, introduction of conductive AgNWs makes it possible to employ this soft actuator in switching control circuits (Fig. 10(b)), rendering it more practical and versatile in application of soft robots and intelligent control systems. Subsequently, Wang and co-workers [142] developed a flexible moisture actuator with an asymmetric sandwich structure by attaching GO to the surface of a PVA-co-PE nanofiber composite containing copper (Cu) nanoparticles (Fig. 10(c)). Based on the special asymmetric structure, the composite shows good response to moisture and infrared light with different bending directions and maintains excellent

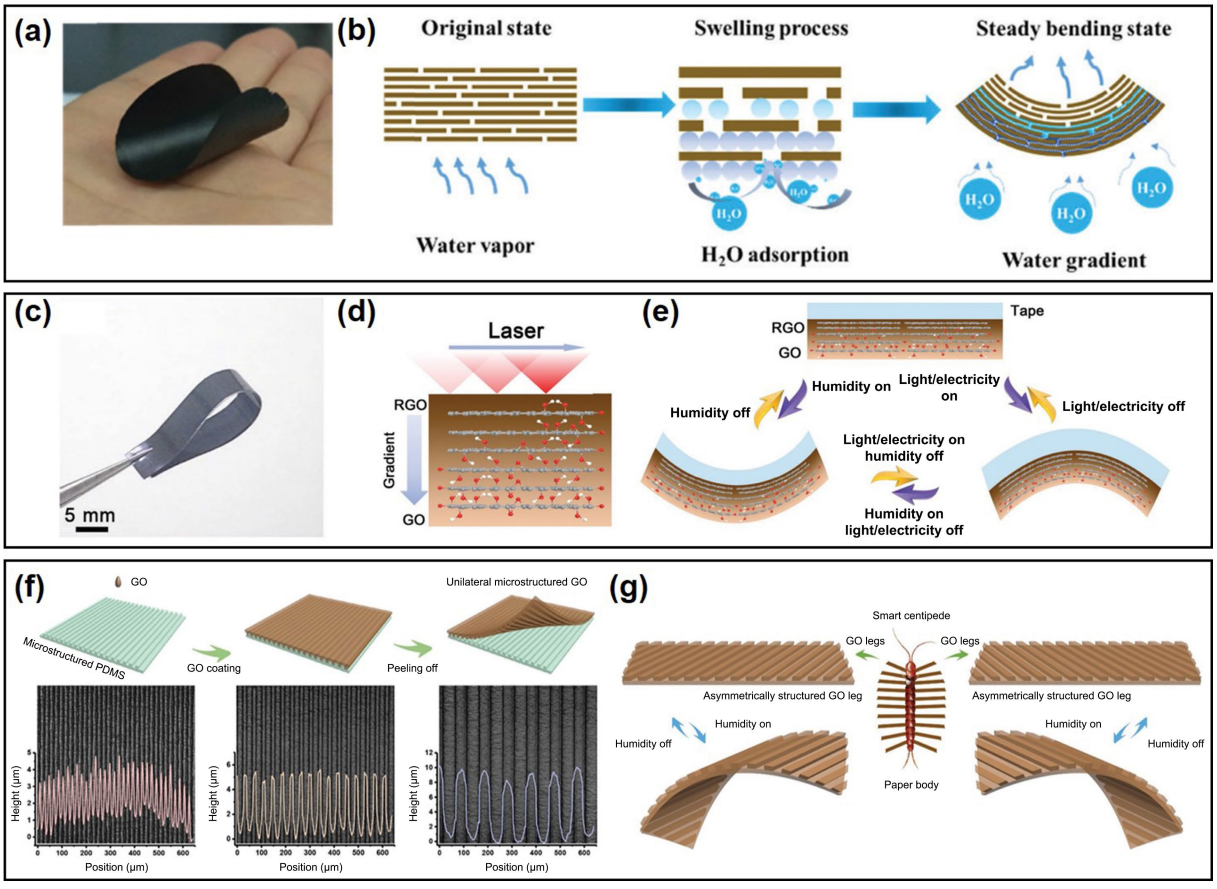

Figure 9 Film moisture actuator based on carbon-based functional material. (a) Photograph of the homogeneous GO film bending upward when placed on the bare palm. (b) Schematic illustration of the locomotion mechanism of the homogeneous GO thin film actuator. Reproduced with permission from Ref. [138], © The Royal Society of Chemistry 2018. (c) The optical photograph of the flexible tape/RGO/GO actuator. (d) The schematic illustration of the lateral reduction gradient of GO under the laser process. (e) The schematic diagram of multi responsive actuation of the tape/RGO/GO trilayer. Reproduced with permission from Ref. [139], © WILEY-VCH Verlag GmbH & Co. KGaA, Weinheim 2019. (f) Schematic illustration of the fabrication and SEM image of structured GO film with periods. (g) Schematic illustration of moisture-responsive smart legs of the centipede mini-robot. Reproduced with permission from Ref. [140], © WILEY-VCH Verlag GmbH & Co. KGaA, Weinheim 2019.

structural stability even after being soaked in water (Fig. 10(d)). This makes it superior to other currently studied moisture-responsive actuation materials.

Above all, a great deal of work has been put into developing moisture-enabled actuators based on the distinctive structures and superior qualities of carbon-based functional materials. These works have attracted a lot of attention and laid the groundwork for future uses of carbon-based functional materials in smart switches, robots, and biomimetic devices.

6 Summary and outlook

Atmospheric moisture holds enormous amounts of water and energy potential, which, with the advancements of nanomaterials, show significant promise in creating circular economies for the current intertwined water and energy challenges. Benefiting from their unique structure and physicochemical properties, carbon-based functional nanomaterials hold great promise as active materials for emerging water and energy harvesting technologies. In this review, progress in advanced technologies such as atmospheric water harvesting, moisture-enabled electricity generation, and moisture-induced deformable actuators based on the interactions between carbon-based functional materials and water molecules in atmospheric moisture is summarized. Although many encouraging advances have been made thanks to the unique properties of carbon-based materials such as good chemical stability, a large specific surface area, a porous structure, ease of functionalization, and good adsorption of moisture, there are still many issues that face practical application needs for improvement (Fig. 11).

For AWH technology, carbon-based functional materials with adjustable structure and excellent properties achieved many great processes in this field. However, pure carbon material shows hydrophobicity, which weakens its interaction with water absorption, hindering the development of its application in water harvesting. The reports appeared so far show that carbon-based functional materials, when combined with other hygroscopic materials and corresponding structure designs, exhibit high water absorption capacity. Hence, future attention should be paid to the design of composites to achieve promising moisture harvesting systems with improved performance.

Besides, based on their excellent properties and easy functionalization as well as variety of assemblies, carbon-based functional materials have been widely used in MEG technology and demonstrated their promise in practical device applications in the construction of self-powered electronics and the incorporation of MEGs in other next-generation devices. Despite these advantages, the power density of MEG is still relatively low and output voltages are typically < 1.5 V. There is then much scope for further development of these devices to improve output power and other output characteristics. Designing porous structures in carbon-based functional materials and further increasing effective surface area may boost the accessibility of water into the materials and improve proton mobility. In addition, introducing a high degree of hydration is also essential to increasing proton conductivity.

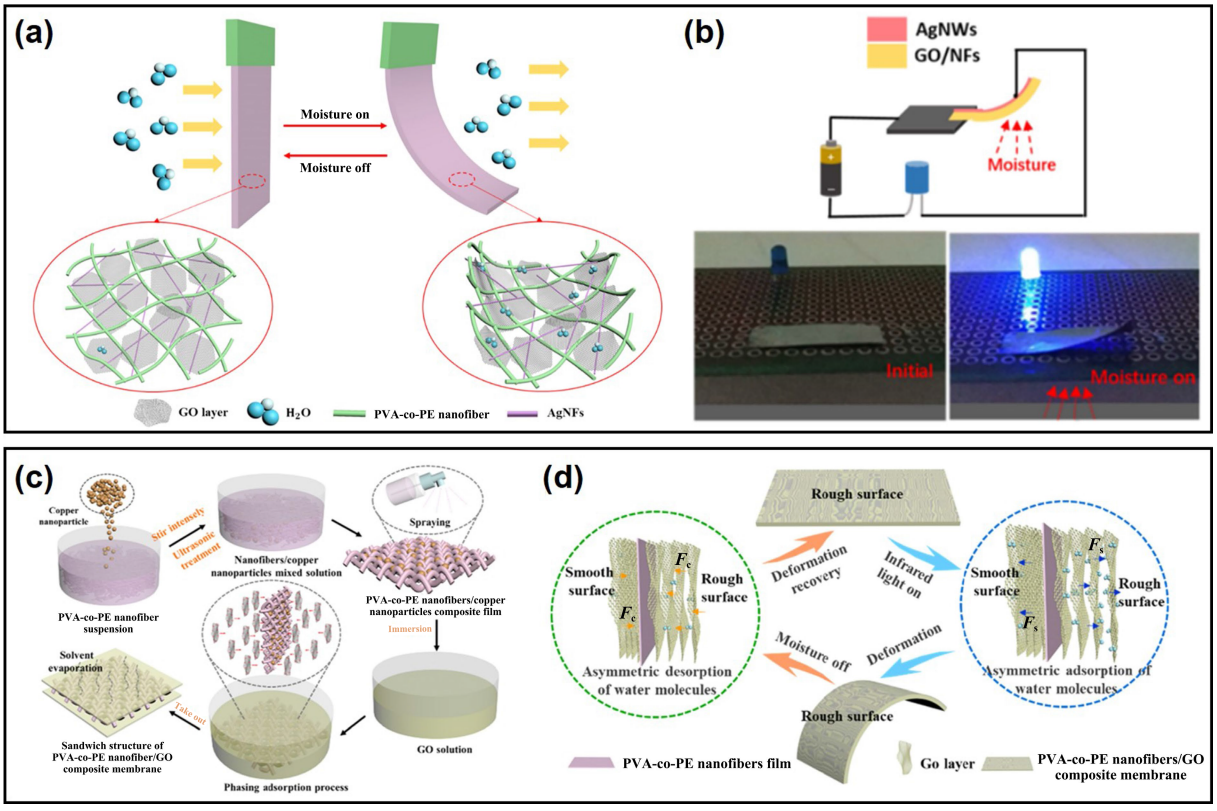

Figure 10 3D network carbon-based functional material for moisture enabled actuator. (a) Schematic diagram of reversible bending behavior of the AgNWs/NFs/GO membrane-based actuator under on/off moisture stimulation. (b) The electrically conductive AgNWs-NFs/GO bilayer membrane can be used as a control switch for the light-emitting diode (LED) lamp under moisture stimulation. Reproduced with permission from Ref. [141], © American Chemical Society 2019. (c) The electrically conductive AgNWs-NFs/GO bilayer membrane can be used as a control switch for the LED lamp under moisture stimulation. (d) Schematic of reversible bending deformation of the Cu@PVA-co-PE/GO composite film stimulated by moisture. Reproduced with permission from Ref. [142], © American Chemical Society 2021.

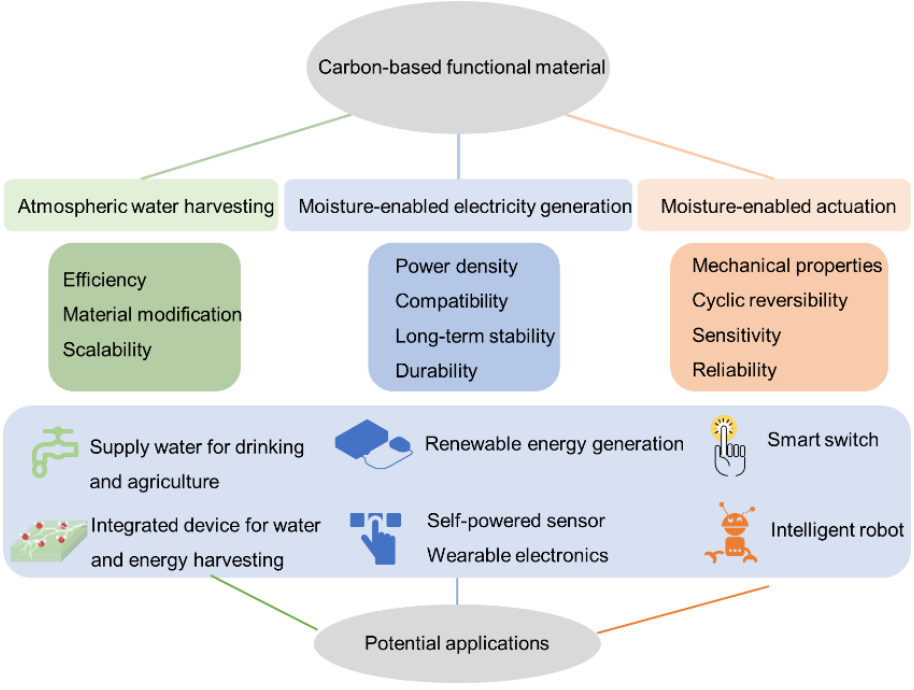

Figure 11 Prospective and challenges of carbon-based functional material for atmospheric moisture utilization.

With its excellent water capture and transfer performance, it is possible to develop an integrated device assembled with carbon functional materials for applications in both water and energy harvesting. For example, this integrated device can find applications in other fields such as environmental monitoring and governance. By collecting water resources and energy, it can provide wireless power to smart monitoring devices, improving convenience and accuracy in environmental monitoring.

Additionally, although some advances in moisture actuators based on carbon functional material were realized, a variety of necessary performance characteristics, such as the mechanical properties and cyclic reversibility of the device, should be considered for its practical application. Consequently, optimizing material selection and scientific structural design for moisture actuators with higher comprehensive performance is needed. Another challenge for carbon functional material-based moisture

actuators is that all the developed techniques for preparing carbon-based macroscopic assemblies face production problems. Thus, a low-cost and large-scale fabrication method for carbon-based macroscopic assemblies with controllable nanostructures is still required to realize practical applications.

In summary, the rapid development of moisture utilization technology based on the interaction between carbon-based functional materials and water molecules in atmospheric moisture has shown fascinating value in addressing the water and energy crises. Although there are still some challenges, we believe that with the continuous development of science, these challenges will be overcome and carbon-based functional materials will be widely applied for water and energy harvesting applications.

Acknowledgements

This work was supported by the National Natural Science Foundation of China (Nos. 52022051, 22035005, 22075165, 52090032, and 52073159), and Tsinghua-Foshan Innovation Special Fund (No. 2020THFS0501).

References

[1] Stephens, G. L.; Li, J.; Wild, M.; Clayson, C. A.; Loeb, N.; Kato, S.; L'Ecuyer, T.; Stackhouse, P. W.; Lebsock, M.; Andrews, T. An update on Earth's energy balance in light of the latest global observations. *Nat. Geosci.* **2012**, *5*, 691–696.

[2] Vörösmarty, C. J.; Mcintyre, P. B.; Gessner, M. O.; Dudgeon, D.; Prusevich, A.; Green, P.; Glidden, S.; Bunn, S. E.; Sullivan, C. A.; Liermann, C. R. et al. Global threats to human water security and river biodiversity. *Nature* **2010**, *467*, 555–561.

[3] Rockström, J.; Mazzucato, M.; Andersen, L. S.; Fahrländer, S. F.; Gerten, D. Why we need a new economics of water as a common good. *Nature* **2023**, *615*, 794–797.

[4] Chu, S.; Majumdar, A. Opportunities and challenges for a sustainable energy future. *Nature* **2012**, *488*, 294–303.

[5] Rodell, M.; Famiglietti, J. S.; Wiese, D. N.; Reager, J. T.; Beaudoing, H. K.; Landerer, F. W.; Lo, M. H. Emerging trends in global freshwater availability. *Nature* **2018**, *557*, 651–659.

[6] Cooley, S. W.; Ryan, J. C.; Smith, L. C. Human alteration of global surface water storage variability. *Nature* **2021**, *591*, 78–81.

[7] Yin, J.; Zhou, J. X.; Fang, S. M.; Guo, W. L. Hydrovoltaic energy on the way. *Joule* **2020**, *4*, 1852–1855.

[8] Lu, W. H.; Ong, W. L.; Ho, G. W. Advances in harvesting water and energy from ubiquitous atmospheric moisture. *J. Mater. Chem. A* **2023**, *11*, 12456–12481.

[9] Wei, Q. M.; Ge, W. N.; Yuan, Z. C.; Wang, S. X.; Lu, C. G.; Feng, S. L.; Zhao, L.; Liu, Y. H. Moisture electricity generation: Mechanisms, structures, and applications. *Nano Res.* **2023**, *16*, 7496–7510.

[10] Wang, K. Q.; Xu, W. H.; Zhang, W.; Wang, X.; Yang, X.; Li, J. F.; Zhang, H. L.; Li, J. J.; Wang, Z. K. Bio-inspired water-driven electricity generators: From fundamental mechanisms to practical applications. *Nano Res. Energy* **2023**, *2*, e9120042.

[11] Han, Y. Y.; Zhang, Z. P.; Qu, L. T. Power generation from graphene–water interactions. *FlatChem* **2019**, *14*, 100090.

[12] Bai, J. X.; Huang, Y. X.; Cheng, H. H.; Qu, L. T. Moist-electric generation. *Nanoscale* **2019**, *11*, 23083–23091.

[13] Wang, H. Y.; Sun, Y. L.; He, T. C.; Huang, Y. X.; Cheng, H. H.; Li, C.; Xie, D.; Yang, P. F.; Zhang, Y. F.; Qu, L. T. Bilayer of polyelectrolyte films for spontaneous power generation in air up to an integrated 1,000 V output. *Nat. Nanotechnol.* **2021**, *16*, 811–819.

[14] Sun, Z. Y.; Wen, X.; Wang, L. M.; Ji, D. X.; Qin, X. H.; Yu, J. Y.; Ramakrishna, S. Emerging design principles, materials, and applications for moisture-enabled electric generation. *eScience* **2022**, *2*, 32–46.

[15] Niklewski, J.; Brischke, C.; Hansson, E. F.; Meyer-Veltrup, L. Moisture behavior of weathered wood surfaces during cyclic wetting: Measurements and modeling. *Wood Sci. Technol.* **2018**, *52*, 1431–1450.

[16] Joffre, T.; Isaksson, P.; Dumont, P. J. J.; Du Roscoat, S. R.; Sticko, S.; Orgéas, L.; Gamstedt, E. K. A method to measure moisture induced swelling properties of a single wood cell. *Exp. Mech.* **2016**, *56*, 723–733.

[17] Brennan, J. K.; Bandosz, T. J.; Thomson, K. T.; Gubbins, K. E. Water in porous carbons. *Colloids Surf. A: Physicochem. Eng. Asp.* **2001**, *187–188*, 539–568.

[18] Zhang, Q.; Xu, W. L.; Wang, X. B. Carbon nanocomposites with high photothermal conversion efficiency. *Sci. China Mater.* **2018**, *61*, 905–914.

[19] Burghaus, U. Adsorption of water on epitaxial graphene. *J. Mater. Res.* **2021**, *36*, 129–139.

[20] Wang, C. Y.; Xing, Y. W.; Lei, Y. Z.; Xia, Y. C.; Zhang, C. H.; Zhang, R.; Wang, S. W.; Chen, P.; Zhu, S.; Li, J. H. et al. Adsorption of water on carbon materials: The formation of "water bridge" and its effect on water adsorption. *Colloids Surf. A: Physicochem. Eng. Asp.* **2021**, *631*, 127719.

[21] Yan, H. L.; Wu, F.; Xue, Y. F.; Bryan, K.; Ma, W. J.; Yu, P.; Mao, L. Q. Water adsorption and transport on oxidized two-dimensional carbon materials. *Chem.—Eur. J.* **2019**, *25*, 3969–3978.

[22] Wang, X.; Kalali, E. N.; Wan, J. T.; Wang, D. Y. Carbon-family materials for flame retardant polymeric materials. *Prog. Polym. Sci.* **2017**, *69*, 22–46.

[23] Novoselov, K. S.; Geim, A. K.; Morozov, S. V.; Jiang, D.; Zhang, Y.; Dubonos, S. V.; Grigorieva, I. V.; Firsov, A. A. Electric field effect in atomically thin carbon films. *Sci. Adv.* **2004**, *306*, 666–669.

[24] Geim, A. K.; Novoselov, K. S. The rise of graphene. *Nat. Mater.* **2007**, *6*, 183–191.

[25] Zhu, Y. W.; Murali, S.; Cai, W. W.; Li, X. S.; Suk, J. W.; Potts, J. R.; Ruoff, R. S. Graphene and graphene oxide: Synthesis, properties, and applications. *Adv. Mater.* **2010**, *22*, 3906–3924.

[26] Lee, C.; Wei, X. D.; Kysar, J. W.; Hone, J. Measurement of the elastic properties and intrinsic strength of monolayer graphene. *Science* **2008**, *321*, 385–388.

[27] Zhang, M.; Yuan, J. Y. Graphene meta-aerogels: When sculpture aesthetic meets 1D/2D composite materials. *Nano Res. Energy* **2022**, *1*, e9120035.

[28] Li, G. X.; Li, Y. L.; Liu, H. B.; Guo, Y. B.; Li, Y. J.; Zhu, D. B. Architecture of graphdiyne nanoscale films. *Chem. Commun.* **2010**, *46*, 3256–3258.

[29] Dalton, A. B.; Collins, S.; Muñoz, E.; Razal, J. M.; Ebron, V. H.; Ferraris, J. P.; Coleman, J. N.; Kim, B. G.; Baughman, R. H. Super-tough carbon-nanotube fibres. *Nature* **2003**, *423*, 703.

[30] Behabtu, N.; Young, C. C.; Tsentalovich, D. E.; Kleinerman, O.; Wang, X.; Ma, A. W. K.; Bengio, E. A.; Ter Waarbeek, R. F.; De Jong, J. J.; Hoogerwerf, R. E. et al. Strong, light, multifunctional fibers of carbon nanotubes with ultrahigh conductivity. *Science* **2013**, *339*, 182–186.

[31] Qian, Q. R.; Sunohara, S.; Kato, Y.; Zaini, M. A. A.; Machida, M.; Tatsumoto, H. Water vapor adsorption onto activated carbons prepared from cattle manure compost (CMC). *Appl. Surf. Sci.* **2008**, *254*, 4868–4874.

[32] Sun, S. N.; Yu, Q. F.; Li, M.; Zhao, H.; Wang, Y. F.; Zhang, Y. Surface modification of porous carbon nanomaterials for water vapor adsorption. *ACS Appl. Nano Mater.* **2023**, *6*, 2822–2834.

[33] Zhang, D. Z.; Pan, W. J.; Tang, M. C.; Wang, D. Y.; Yu, S. J.; Mi, Q.; Pan, Q. N.; Hu, Y. Q. Diversiform gas sensors based on two-dimensional nanomaterials. *Nano Res.*, in press, https://doi.org/10.1007/s12274-022-5233-2.

[34] Liu, X.; Dai, L. M. Carbon-based metal-free catalysts. *Nat. Rev. Mater.* **2016**, *1*, 16064.

[35] Ding, X. T.; Niu, Y. S.; Zhang, G.; Xu, Y. H.; Li, J. H. Electrochemistry in carbon-based quantum dots. *Chem. Asian J.* **2020**, *15*, 1214–1224.

[36] Chen, S.; Chen, Q. W.; Ding, S. Y.; Tian, Y. D.; Wang, J.; Hou, S. Q.; Zhang, J. T. Rational design of carbon-based electrocatalysts for enhancing redox reactions in rechargeable metal batteries. *Nano Res.* **2023**, *16*, 4246–4276.

[37] Lan, G. J.; Yang, J.; Ye, R. P.; Boyjoo, Y.; Liang, J.; Liu, X. Y.; Li, Y.; Liu, J.; Qian, K. Sustainable carbon materials toward emerging applications. *Small Methods* **2021**, *5*, 2001250.

[38] Chen, Y. P.; Wei, J. T.; Duyar, M. S.; Ordomsky, V. V.; Khodakov, A. Y.; Liu, J. Carbon-based catalysts for fischer-tropsch synthesis. *Chem. Soc. Rev.* **2021**, *50*, 2337–2366.

[39] Zhang, H. M.; Liu, W. H.; Cao, D.; Cheng, D. J. Carbon-based material-supported single-atom catalysts for energy conversion. *iScience* **2022**, *25*, 104367.

[40] Shang, H. S.; Liu, D. Atomic design of carbon-based dual-metal site catalysts for energy applications. *Nano Res.* **2023**, *16*, 6477–6506.

[41] Ma, Q. L.; Yu, Y. F.; Sindoro, M.; Fane, A. G.; Wang, R.; Zhang, H. Carbon-based functional materials derived from waste for water remediation and energy storage. *Adv. Mater.* **2017**, *29*, 1605361.

[42] Ibrahim, H.; Sazali, N.; Salleh, W. N. W.; Ngadiman, N. H. A.; Fadil, N. A.; Harun, Z. Outlook on the carbon-based materials for heavy metal removal. *Biointerface Res. Appl. Chem.* **2021**, *12*, 5303–5323.

[43] Abbo, H. S.; Gupta, K. C.; Khaligh, N. G.; Titinchi, S. J. J. Carbon nanomaterials for wastewater treatment. *ChemBioEng Rev.* **2021**, *8*, 463–489.

[44] Hu, Y. J.; Yao, H. Z.; Liao, Q. H.; Lin, T. Y.; Cheng, H. H.; Qu, L. T. The promising solar-powered water purification based on graphene functional architectures. *EcoMat* **2022**, *4*, e12205.

[45] Teradal, N. L.; Jelinek, R. Carbon nanomaterials in biological studies and biomedicine. *Adv. Healthc. Mater.* **2017**, *6*, 1700574.

[46] Wang, J.; Xin, H. L.; Wang, D. L. Recent progress on mesoporous carbon materials for advanced energy conversion and storage. *Part. Part. Syst. Charact.* **2014**, *31*, 515–539.

[47] Zhong, X. W.; Wu, Y.; Zeng, S. F.; Yu, Y. Carbon and carbon hybrid materials as anodes for sodium-ion batteries. *Chem. Asian J.* **2018**, *13*, 1248–1265.

[48] Zhang, L. L.; Wang, Y. J.; Niu, Z. Q.; Chen, J. Advanced nanostructured carbon-based materials for rechargeable lithium-sulfur batteries. *Carbon* **2019**, *141*, 400–416.

[49] Zhang, Y. C.; Zhang, Q. C.; Chen, G. M. Carbon and carbon composites for thermoelectric applications. *Carbon Energy* **2020**, *2*, 408–436.

[50] Wang, Z. T.; Zhang, M. Q.; Ma, W. T.; Zhu, J. B.; Song, W. X. Application of carbon materials in aqueous zinc ion energy storage devices. *Small* **2021**, *17*, 2100219.

[51] Gao, X. Y.; Li, J. F.; Zuo, Z. C. Advanced electrochemical energy storage and conversion on graphdiyne interface. *Nano Res. Energy* **2022**, *1*, e9120036.

[52] Wang, P. F.; Dai, X.; Xu, P.; Hu, S. J.; Xiong, X. Y.; Zou, K. Y.; Guo, S. W.; Sun, J. J.; Zhang, C. F.; Liu, Y. N. et al. Hierarchical and lamellar porous carbon as interconnected sulfur host and polysulfide-proof interlayer for Li-S batteries. *eScience* **2023**, *3*, 100088.

[53] Zheng, Y. T.; Wei, J. J.; Liu, J. L.; Chen, L. X.; An, K.; Zhang, X. T.; Ye, H. T.; Ouyang, X. P.; Li, C. M. Carbon materials: The burgeoning promise in electronics. *Int. J. Miner. Metall Mater.* **2022**, *29*, 404–423.

[54] Cai, X.; Wang, S.; Peng, L. M. Recent progress of photodetector based on carbon nanotube film and application in optoelectronic integration. *Nano Res. Energy* **2023**, *2*, e9120058.

[55] Rodriguez-Reinoso, F.; Molina-Sabio, M.; Muñecas, M. A. Effect of microporosity and oxygen surface groups of activated carbon in the adsorption of molecules of different polarity. *J. Phys. Chem.* **1992**, *96*, 2707–2713.

[56] Picaud, S.; Collignon, B.; Hoang, P. N. M.; Rayez, J. C. Adsorption of water molecules on partially oxidized graphite surfaces: A molecular dynamics study of the competition between OH and COOH sites. *Phys. Chem. Chem. Phys.* **2008**, *10*, 6998–7009.

[57] Miura, K.; Morimoto, T. Adsorption sites for water on graphite. 6. Effect of ozone treatment of sample. *Langmuir* **1994**, *10*, 807–811.

[58] Fletcher, A. J.; Uygur, Y.; Thomas, K. M. Role of surface functional groups in the adsorption kinetics of water vapor on microporous activated carbons. *J. Phys. Chem. C* **2007**, *111*, 8349–8359.

[59] Nguyen, V. T.; Horikawa, T.; Do, D. D.; Nicholson, D. Water as a potential molecular probe for functional groups on carbon surfaces. *Carbon* **2014**, *67*, 72–78.

[60] Klomkliang, N.; Kaewmanee, R.; Saimoey, S.; Intarayothya, S.; Do, D. D.; Nicholson, D. Adsorption of water and methanol on highly graphitized thermal carbon black: The effects of functional group and temperature on the isosteric heat at low loadings. *Carbon* **2016**, *99*, 361–369.

[61] Zeng, Y. H.; Prasetyo, L.; Nguyen, V. T.; Horikawa, T.; Do, D. D.; Nicholson, D. Characterization of oxygen functional groups on carbon surfaces with water and methanol adsorption. *Carbon* **2015**, *81*, 447–457.

[62] Liu, L. M.; Tan, S. J.; Horikawa, T.; Do, D. D.; Nicholson, D.; Liu, J. J. Water adsorption on carbon—A review. *Adv. Colloid Interface Sci.* **2017**, *250*, 64–78.

[63] Ohta, N.; Nishi, Y.; Morishita, T.; Ieko, Y.; Ito, A.; Inagaki, M. Preparation of microporous carbon foams for adsorption/desorption of water vapor in ambient air. *New Carbon Mater.* **2008**, *23*, 216–220.

[64] Striolo, A.; Chialvo, A. A.; Cummings, P. T.; Gubbins, K. E. Water adsorption in carbon-slit nanopores. *Langmuir* **2003**, *19*, 8583–8591.

[65] Horikawa, T.; Muguruma, T.; Do, D. D.; Sotowa, K. I.; Alcántara-Avila, J. R. Scanning curves of water adsorption on graphitized thermal carbon black and ordered mesoporous carbon. *Carbon* **2015**, *95*, 137–143.

[66] Liu, L. M.; Zeng, Y. H.; Tan, S. J.; Xu, H.; Do, D. D.; Nicholson, D.; Liu, J. J. On the mechanism of water adsorption in carbon micropores—A molecular simulation study. *Chem. Eng. J.* **2019**, *357*, 358–366.

[67] LaPotin, A.; Kim, H.; Rao, S. R.; Wang, E. N. Adsorption-based atmospheric water harvesting: Impact of material and component properties on system-level performance. *Acc. Chem. Res.* **2019**, *52*, 1588–1597.

[68] Zhou, X. Y.; Lu, H. Y.; Zhao, F.; Yu, G. H. Atmospheric water harvesting: A review of material and structural designs. *ACS Mater. Lett.* **2020**, *2*, 671–684.

[69] Lu, H. Y.; Shi, W.; Guo, Y. H.; Guan, W. X.; Lei, C. X.; Yu, G. H. Materials engineering for atmospheric water harvesting: Progress and perspectives. *Adv. Mater.* **2022**, *34*, 2110079.

[70] Shi, W.; Guan, W. X.; Lei, C. X.; Yu, G. H. Sorbents for atmospheric water harvesting: From design principles to applications. *Angew. Chem., Int. Ed.* **2022**, *61*, e202211267.

[71] Lian, B.; De Luca, S.; You, Y.; Alwarappan, S.; Yoshimura, M.; Sahajwalla, V.; Smith, S. C.; Leslie, G.; Joshi, R. K. Extraordinary water adsorption characteristics of graphene oxide. *Chem. Sci.* **2018**, *9*, 5106–5111.

[72] Yang, K. J.; Pan, T. T.; Pinnau, I.; Shi, Z.; Han, Y. Simultaneous generation of atmospheric water and electricity using a hygroscopic aerogel with fast sorption kinetics. *Nano Energy* **2020**, *78*, 105326.

[73] Anjali, C.; Renuka, N. K. Atmospheric water harvesting: Prospectus on graphene-based materials. *J. Mater. Res.* **2022**, *37*, 2227–2240.

[74] Huang, Y. W.; Yu, Q. F.; Li, M.; Jin, S. X.; Fan, J.; Zhao, L.; Yao, Z. H. Surface modification of activated carbon fiber by low-temperature oxygen plasma: Textural property, surface chemistry, and the effect of water vapor adsorption. *Chem. Eng. J.* **2021**, *418*, 129474.

[75] Xiao, J.; Liu, Z. L.; Kim, K.; Chen, Y. S.; Yan, J.; Li, Z.; Wang, W. L. S/O-functionalities on modified carbon materials governing adsorption of water vapor. *J. Phys. Chem. C* **2013**, *117*, 23057–23065.

[76] Li, R. Y.; Shi, Y.; Alsaedi, M.; Wu, M. C.; Shi, L.; Wang, P. Hybrid hydrogel with high water vapor harvesting capacity for deployable solar-driven atmospheric water generator. *Environ. Sci. Technol.* **2018**, *52*, 11367–11377.

[77] Li, R. Y.; Shi, Y.; Shi, L.; Alsaedi, M.; Wang, P. Harvesting water from air: Using anhydrous salt with sunlight. *Environ. Sci. Technol.* **2018**, *52*, 5398–5406.

[78] Chen, B.; Zhao, X.; Yang, Y. Superelastic graphene nanocomposite for high cycle-stability water capture-release under sunlight. *ACS Appl. Mater. Interfaces* **2019**, *11*, 15616–15622.

[79] Wang, X. Y.; Li, X. Q.; Liu, G. L.; Li, J. L.; Hu, X. Z.; Xu, N.; Zhao, W.; Zhu, B.; Zhu, J. An interfacial solar heating assisted liquid sorbent atmospheric water generator. *Angew. Chem., Int. Ed.* **2019**, *58*, 12054–12058.
[80] Hou, Y. L.; Sheng, Z. Z.; Fu, C.; Kong, J.; Zhang, X. T. Hygroscopic holey graphene aerogel fibers enable highly efficient moisture capture, heat allocation and microwave absorption. *Nat. Commun.* **2022**, *13*, 1227.
[81] Hu, Y.; Fang, Z.; Wan, X. Y.; Ma, X.; Wang, S. L.; Fan, S. K.; Dong, M. Y.; Ye, Z. Z.; Peng, X. S. Carbon nanotubes decorated hollow metal-organic frameworks for efficient solar-driven atmospheric water harvesting. *Chem. Eng. J.* **2022**, *430*, 133086.
[82] Song, Y.; Xu, N.; Liu, G. L.; Qi, H. S.; Zhao, W.; Zhu, B.; Zhou, L.; Zhu, J. High-yield solar-driven atmospheric water harvesting of metal-organic-framework-derived nanoporous carbon with fast-diffusion water channels. *Nat. Nanotechnol.* **2022**, *17*, 857–863.
[83] Ishii, A.; Machiya, H.; Kato, Y. K. High efficiency dark-to-bright exciton conversion in carbon nanotubes. *Phys. Rev. X* **2019**, *9*, 041048.
[84] Liu, H. C.; Huang, G. C.; Wang, R.; Huang, L.; Wang, H. Z.; Hu, Y. Z.; Cong, G. T.; Bao, F.; Xu, M.; Zhu, C. Z. et al. Carbon nanotubes grown on the carbon fibers to enhance the photothermal conversion toward solar-driven applications. *ACS Appl. Mater. Interfaces* **2022**, *14*, 32404–32411.
[85] Yao, H. Z.; Zhang, P. P.; Huang, Y. X.; Cheng, H. H.; Li, C.; Qu, L. T. Highly efficient clean water production from contaminated air with a wide humidity range. *Adv. Mater.* **2020**, *32*, 1905875.
[86] Xu, J. X.; Li, T. X.; Yan, T. S.; Wu, S.; Wu, M. Q.; Chao, J. W.; Huo, X. Y.; Wang, P. F.; Wang, R. Z. Ultrahigh solar-driven atmospheric water production enabled by scalable rapid-cycling water harvester with vertically aligned nanocomposite sorbent. *Energy Environ. Sci.* **2021**, *14*, 5979–5994.
[87] Zhang, Y. X.; Nandakumar, D. K.; Tan, S. C. Digestion of ambient humidity for energy generation. *Joule* **2020**, *4*, 2532–2536.
[88] Guan, P. Y.; Zhu, R. B.; Hu, G. Y.; Patterson, R.; Chen, F. D.; Liu, C.; Zhang, S.; Feng, Z. H.; Jiang, Y.; Wan, T. et al. Recent development of moisture-enabled-electric nanogenerators. *Small* **2022**, *18*, 2204603.
[89] Wang, P. F.; Xu, J. X.; Wang, R. Z.; Li, T. X. Pathways for continuous electricity generation from ambient moisture. *Matter* **2023**, *6*, 19–22.
[90] Li, M. J.; Zong, L.; Yang, W. Q.; Li, X. K.; You, J.; Wu, X. C.; Li, Z. H.; Li, C. X. Biological nanofibrous generator for electricity harvest from moist air flow. *Adv. Funct. Mater.* **2019**, *29*, 1901798.
[91] Shen, D. Z.; Xiao, M.; Zou, G. S.; Liu, L.; Duley, W. W.; Zhou, Y. N. Self-powered wearable electronics based on moisture enabled electricity generation. *Adv. Mater.* **2018**, *30*, 1705925.
[92] Tan, J.; Fang, S. M.; Zhang, Z. H.; Yin, J.; Li, L. X.; Wang, X.; Guo, W. L. Self-sustained electricity generator driven by the compatible integration of ambient moisture adsorption and evaporation. *Nat. Commun.* **2022**, *13*, 3643.
[93] Zhao, F.; Cheng, H. H.; Zhang, Z. P.; Jiang, L.; Qu, L. T. Direct power generation from a graphene oxide film under moisture. *Adv. Mater.* **2015**, *27*, 4351–4357.
[94] Huang, Y. X.; Cheng, H. H.; Shi, G. Q.; Qu, L. T. Highly efficient moisture-triggered nanogenerator based on graphene quantum dots. *ACS Appl. Mater. Interfaces* **2017**, *9*, 38170–38175.
[95] Li, Q. J.; Zhou, M.; Yang, Q. F.; Yang, M. Y.; Wu, Q.; Zhang, Z. X.; Yu, J. W. Flexible carbon dots composite paper for electricity generation from water vapor absorption. *J. Mater. Chem. A* **2018**, *6*, 10639–10643.
[96] Liang, Y.; Zhao, F.; Cheng, Z. H.; Zhou, Q. H.; Shao, H. B.; Jiang, L.; Qu, L. T. Self-powered wearable graphene fiber for information expression. *Nano Energy* **2017**, *32*, 329–335.
[97] Zhao, F.; Wang, L. X.; Zhao, Y.; Qu, L. T.; Dai, L. M. Graphene oxide nanoribbon assembly toward moisture-powered information storage. *Adv. Mater.* **2017**, *29*, 1604972.
[98] Shao, C. X.; Gao, J.; Xu, T.; Ji, B. X.; Xiao, Y. K.; Gao, C.; Zhao, Y.; Qu, L. T. Wearable fiberform hygroelectric generator. *Nano Energy* **2018**, *53*, 698–705.
[99] Sun, Z. Y.; Feng, L. L.; Xiong, C. D.; He, X. Y.; Wang, L. M.; Qin, X. H.; Yu, J. Y. Electrospun nanofiber fabric: An efficient, breathable and wearable moist-electric generator. *J. Mater. Chem. A* **2021**, *9*, 7085–7093.
[100] He, W. Y.; Wang, H. Y.; Huang, Y. X.; He, T. C.; Chi, F. Y.; Cheng, H. H.; Liu, D.; Dai, L. M.; Qu, L. T. Textile-based moisture power generator with dual asymmetric structure and high flexibility for wearable applications. *Nano Energy* **2022**, *95*, 107017.
[101] Hu, K. S.; Xiong, R.; Guo, H. Y.; Ma, R. L.; Zhang, S. D.; Wang, Z. L.; Tsukruk, V. V. Self-powered electronic skin with biotactile selectivity. *Adv. Mater.* **2016**, *28*, 3549–3556.
[102] Liu, K.; Yang, P. H.; Li, S.; Li, J.; Ding, T. P.; Xue, G. B.; Chen, Q.; Feng, G.; Zhou, J. Induced potential in porous carbon films through water vapor absorption. *Angew. Chem., Int. Ed.* **2016**, *55*, 8003–8007.
[103] Cheng, H. H.; Huang, Y. X.; Qu, L. T.; Cheng, Q. L.; Shi, G. Q.; Jiang, L. Flexible in-plane graphene oxide moisture-electric converter for touchless interactive panel. *Nano Energy* **2018**, *45*, 37–43.
[104] Xu, T.; Ding, X. T.; Shao, C. X.; Song, L.; Lin, T. Y.; Gao, X.; Xue, J. L.; Zhang, Z. P.; Qu, L. T. Electric power generation through the direct interaction of pristine graphene-oxide with water molecules. *Small* **2018**, *14*, 1704473.
[105] Lee, S.; Jang, H.; Lee, H.; Yoon, D.; Jeon, S. Direct fabrication of a moisture-driven power generator by laser-induced graphitization with a gradual defocusing method. *ACS Appl. Mater. Interfaces* **2019**, *11*, 26970–26975.
[106] Liang, Y.; Zhao, F.; Cheng, Z. H.; Deng, Y. X.; Xiao, Y. K.; Cheng, H. H.; Zhang, P. P.; Huang, Y. X.; Shao, H. B.; Qu, L. T. Electric power generation via asymmetric moisturizing of graphene oxide for flexible, printable and portable electronics. *Energ. Environ. Sci.* **2018**, *11*, 1730–1735.
[107] Luo, Z. L.; Liu, C. H.; Fan, S. S. A moisture induced self-charging device for energy harvesting and storage. *Nano Energy* **2019**, *60*, 371–376.
[108] Yang, C.; Huang, Y. X.; Cheng, H. H.; Jiang, L.; Qu, L. T. Rollable, stretchable, and reconfigurable graphene hygroelectric generators. *Adv. Mater.* **2019**, *31*, 1805705.
[109] Zhang, B. X.; Wang, K. X.; Ji, X.; Wang, S. Y.; Ma, Z.; Qiu, Y. F. A self-powered moisture detector using graphene oxide film constructed by asymmetric metal electrodes. *J. Alloys Compd.* **2019**, *810*, 151880.
[110] Li, Z. X.; Wang, J.; Dai, L.; Sun, X. H.; An, M.; Duan, C.; Li, J.; Ni, Y. H. Asymmetrically patterned cellulose nanofibers/graphene oxide composite film for humidity sensing and moist-induced electricity generation. *ACS Appl. Mater. Interfaces* **2020**, *12*, 55205–55214.
[111] Chen, S.; Xia, H.; Ni, Q. Q. A wearable sustainable moisture-induced electricity generator based on rGO/GO/rGO sandwich-like structural film. *Adv. Electron. Mater.* **2021**, *7*, 2100222.
[112] Lei, D. D.; Zhang, Q. X.; Liu, N. S.; Su, T. Y.; Wang, L. X.; Ren, Z. Q.; Zhang, Z.; Su, J.; Gao, Y. H. Self-powered graphene oxide humidity sensor based on potentiometric humidity transduction mechanism. *Adv. Funct. Mater.* **2022**, *32*, 2107330.
[113] Chen, S.; Xia, H.; Ni, Q. Q. A sustainable, continuously expandable, wearable breath moisture-induced electricity generator. *Carbon* **2022**, *194*, 104–113.
[114] Faramarzi, P.; Kim, B.; You, J. B.; Jeong, S. H. CNT-functionalized electrospun fiber mat for a stretchable moisture-driven power generator. *J. Mater. Chem. C* **2023**, *11*, 2206–2216.
[115] Zhao, F.; Liang, Y.; Cheng, H. H.; Jiang, L.; Qu, L. T. Highly efficient moisture-enabled electricity generation from graphene oxide frameworks. *Energy Environ. Sci.* **2016**, *9*, 912–916.
[116] Cheng, H. H.; Huang, Y. X.; Zhao, F.; Yang, C.; Zhang, P. P.; Jiang, L.; Shi, G. Q.; Qu, L. T. Spontaneous power source in ambient air of a well-directionally reduced graphene oxide bulk. *Energy Environ. Sci.* **2018**, *11*, 2839–2845.
[117] Huang, Y. X.; Cheng, H. H.; Yang, C.; Zhang, P. P.; Liao, Q. H.; Yao, H. Z.; Shi, G. Q.; Qu, L. T. Interface-mediated hygroelectric generator with an output voltage approaching 1.5 volts. *Nat. Commun.* **2018**, *9*, 4166.
[118] Huang, Y. X.; Cheng, H. H.; Yang, C.; Yao, H. Z.; Li, C.; Qu, L. T.

All-region-applicable, continuous power supply of graphene oxide composite. *Energ. Environ. Sci.* **2019**, *12*, 1848–1856.
[119] Fan, K.; Liu, X. K.; Liu, Y.; Li, Y.; Liu, X. Y.; Feng, W.; Wang, X. Spontaneous power generation from broad-humidity atmospheres through heterostructured F/O-bonded graphene monoliths. *Nano Energy* **2022**, *91*, 106605.
[120] Yang, C.; Wang, H. Y.; Bai, J. X.; He, T. C.; Cheng, H. H.; Guang, T. L.; Yao, H. Z.; Qu, L. T. Transfer learning enhanced water-enabled electricity generation in highly oriented graphene oxide nanochannels. *Nat. Commun.* **2022**, *13*, 6819.
[121] Han, B.; Zhang, Y. L.; Chen, Q. D.; Sun, H. B. Carbon-based photothermal actuators. *Adv. Funct. Mater.* **2018**, *28*, 1802235.
[122] Zheng, Q. C.; Xu, C. X.; Jiang, Z. L.; Zhu, M.; Chen, C.; Fu, F. F. Smart actuators based on external stimulus response. *Front. Chem.* **2021**, *9*, 650358.
[123] Chi, Y. D.; Li, Y. B.; Zhao, Y.; Hong, Y. Y.; Tang, Y. C.; Yin, J. Bistable and multistable actuators for soft robots: Structures, materials, and functionalities. *Adv. Mater.* **2022**, *34*, 2110384.
[124] Li, M.; Pal, A.; Aghakhani, A.; Pena-Francesch, A.; Sitti, M. Soft actuators for real-world applications. *Nat. Rev. Mater.* **2022**, *7*, 235–249.
[125] Wang, M. T.; Li, Q. C.; Shi, J. X.; Cao, X. Y.; Min, L. Z.; Li, X. F.; Zhu, L. L.; Lv, Y. H.; Qin, Z.; Chen, X. Y. et al. Bio-inspired high sensitivity of moisture-mechanical go films with period-gradient structures. *ACS Appl. Mater. Interfaces* **2020**, *12*, 33104–33112.
[126] Van Opdenbosch, D.; Fritz-Popovski, G.; Wagermaier, W.; Paris, O.; Zollfrank, C. Moisture-driven ceramic bilayer actuators from a biotemplating approach. *Adv. Mater.* **2016**, *28*, 5235–5240.
[127] Mao, J. W.; Chen, Z. D.; Han, D. D.; Ma, J. N.; Zhang, Y. L.; Sun, H. B. Nacre-inspired moisture-responsive graphene actuators with robustness and self-healing properties. *Nanoscale* **2019**, *11*, 20614–20619.
[128] Liu, Y. Q.; Chen, Z. D.; Han, D. D.; Mao, J. W.; Ma, J. N.; Zhang, Y. L.; Sun, H. B. Bioinspired soft robots based on the moisture-responsive graphene oxide. *Adv. Sci. (Weinh.)* **2021**, *8*, 2002464.
[129] Yang, L. Y.; Cui, J.; Zhang, L.; Xu, X. R.; Chen, X.; Sun, D. P. A moisture-driven actuator based on polydopamine-modified MXene/bacterial cellulose nanofiber composite film. *Adv. Funct. Mater.* **2021**, *31*, 2101378.
[130] Li, J. J.; Zhang, G. H.; Cui, Z. P.; Bao, L. L.; Xia, Z. G.; Liu, Z. F.; Zhou, X. High performance and multifunction moisture-driven yin–yang-interface actuators derived from polyacrylamide hydrogel. *Small*, in press, https://doi.org/10.1002/SMLL.202303228.
[131] Cheng, H. H.; Liu, J.; Zhao, Y.; Hu, C. G.; Zhang, Z. P.; Chen, N.; Jiang, L.; Qu, L. T. Graphene fibers with predetermined deformation as moisture-triggered actuators and robots. *Angew. Chem., Int. Ed.* **2013**, *52*, 10482–10486.
[132] Cheng, H. H.; Hu, Y.; Zhao, F.; Dong, Z. L.; Wang, Y. H.; Chen, N.; Zhang, Z. P.; Qu, L. T. Moisture-activated torsional graphene-fiber motor. *Adv. Mater.* **2014**, *26*, 2909–2913.
[133] He, S. S.; Chen, P. N.; Qiu, L. B.; Wang, B. J.; Sun, X. M.; Xu, Y. F.; Peng, H. S. A mechanically actuating carbon-nanotube fiber in response to water and moisture. *Angew. Chem., Int. Ed.* **2015**, *54*, 14880–14884.
[134] Gu, X. G.; Fan, Q. X.; Yang, F.; Cai, L.; Zhang, N.; Zhou, W. B.; Zhou, W. Y.; Xie, S. S. Hydro-actuation of hybrid carbon nanotube yarn muscles. *Nanoscale* **2016**, *8*, 17881–17886.
[135] Kim, S. H.; Kwon, C. H.; Park, K.; Mun, T. J.; Lepró, X.; Baughman, R. H.; Spinks, G. M.; Kim, S. J. Bio-inspired, moisture-powered hybrid carbon nanotube yarn muscles. *Sci. Rep.* **2016**, *6*, 23016.
[136] Park, S.; An, J.; Suk, J. W.; Ruoff, R. S. Graphene-based actuators. *Small* **2010**, *6*, 210–212.
[137] Cheng, H. H.; Zhao, F.; Xue, J. L.; Shi, G. Q.; Jiang, L.; Qu, L. T. One single graphene oxide film for responsive actuation. *ACS Nano* **2016**, *10*, 9529–9535.
[138] Ge, Y. H.; Cao, R.; Ye, S. J.; Chen, Z.; Zhu, Z. F.; Tu, Y. F.; Ge, D. T.; Yang, X. M. A bio-inspired homogeneous graphene oxide actuator driven by moisture gradients. *Chem. Commun.* **2018**, *54*, 3126–3129.
[139] Ma, J. N.; Mao, J. W.; Han, D. D.; Fu, X. Y.; Wang, Y. X.; Zhang, Y. L. Laser programmable patterning of rGO/GO janus paper for multiresponsive actuators. *Adv. Mater. Technol,* **2019**, *4*, 1900554.
[140] Zhang, Y. L.; Liu, Y. Q.; Han, D. D.; Ma, J. N.; Wang, D.; Li, X. B.; Sun, H. B. Quantum-confined-superfluidics-enabled moisture actuation based on unilaterally structured graphene oxide papers. *Adv. Mater.* **2019**, *31*, 1901585.
[141] Xiang, C. X.; Wang, W.; Zhu, Q.; Xue, D.; Zhao, X.; Li, M. F.; Wang, D. Flexible and super-sensitive moisture-responsive actuators by dispersing graphene oxide into three-dimensional structures of nanofibers and silver nanowires. *ACS Appl. Mater. Interfaces* **2020**, *12*, 3245–3253.
[142] Wang, W.; Wang, S.; Xiang, C. X.; Liu, S. Y.; Li, M. F.; Wang, D. Graphene oxide/nanofiber-based actuation films with moisture and photothermal stimulation response for remote intelligent control applications. *ACS Appl. Mater. Interfaces* **2021**, *13*, 48179–48188.
[143] Lv, Y. H.; Li, Q. C.; Shi, J. X.; Qin, Z.; Lei, Q. J.; Zhao, B.; Zhu, L. L.; Pan, K. Graphene-based moisture actuator with oriented microstructures prepared by one-step laser reduction for accurately controllable responsive direction and position. *ACS Appl. Mater. Interfaces* **2022**, *14*, 12434–12441.